

Coherent Ultrafast Optical Dynamics of the Fermi Edge Singularity

N. Primozich, T. V. Shahbazyan, and I. E. Perakis

Department of Physics and Astronomy, Vanderbilt University, Nashville, TN 37235

D. S. Chemla

*Department of Physics, University of California, Berkeley, CA 94720 and Materials Science
Division, Lawrence Berkeley National Laboratory, Berkeley, CA 94720*

Abstract

We develop a non-equilibrium many-body theory of the coherent femtosecond nonlinear optical response of the Fermi edge singularity. We study the role of the dynamical Fermi sea response in the time-evolution of the pump-probe spectra. The electron-hole correlations are treated nonperturbatively with the time-dependent coupled cluster expansion combined with the effective Hamiltonian approach. For short pulse durations, we find a non-exponential decay of the differential transmission during negative time delays, which is governed by the interactions. This is in contrast to the results obtained within the Hartree-Fock approximation, which predicts an exponential decay governed by the dephasing time. We discuss the role of the optically-induced dephasing effects in the coherent regime.

PACS numbers: 71.10.Ca, 71.45.-d, 78.20.Bh, 78.47.+p

arXiv:cond-mat/9908105v4 4 Oct 1999

I. INTRODUCTION

Ultrafast nonlinear spectroscopy provides unique and powerful tools for studying the dynamics of Coulomb correlation effects in semiconductors, since the time resolution can now be much smaller than the scattering times of the elementary excitations and, e.g, the period of optical phonons or plasmons. During the past decade, femtosecond pump-probe and wave-mixing experiments have demonstrated that in these materials both coherent and dissipative processes are governed by many-body effects.¹ Parallel theoretical advances have accounted for the two-particle correlation effects in undoped semiconductors through the time dependent Hartree-Fock approximation (HFA), which has developed into the very successful Semiconductor Bloch Equations (SBE's) formalism.²⁻⁴ However, more recent experimental observations could not be explained within this mean field approach and were attributed to four-particle and higher order Coulomb correlation effects.⁵⁻⁸ These high order correlation effects have been mostly studied with equation-of-motion methods for density matrices⁹⁻¹¹ or pair-operators¹² and by using the Keldysh Green's function formalism.¹³

At the same time, much less is known about the role of *coherent* many-body effects in the nonlinear optical response of doped semiconductors and, in particular, modulation-doped heterostructures. Some aspects of the effects of the electron-electron ($e-e$) scattering have been described within the dephasing and relaxation time approximations without microscopic justification. Most importantly however, the role of the time-dependent electron-hole ($e-h$) correlations between the photoexcited holes and the Fermi sea (FS) electrons on the ultrafast dynamics is still poorly understood. The main difficulty comes from the non-perturbative nature of the Fermi edge singularity (FES) which dominates the absorption spectrum close to the absorption onset, and which cannot be described within the above approximations.^{14,15} Important here is that the $e-h$ interactions between a heavy photoexcited hole and the FS-electrons lead to the scattering of a macroscopic number of low-energy FS-pairs, which readjusts the entire FS into a new orthogonal scattering state in the course of the optical excitation (Anderson orthogonality catastrophe¹⁶).

The FES is a many-body resonance that has been observed both in doped semiconductors and in metals.^{14,17,18} Its non-Lorentzian lineshape can be viewed as originating from the decay of an excitonic bound state caused by its interactions with the gapless FS excitations.¹⁵ In a first approximation, the excitonic effects in a doped semiconductor can be described by extending the mean field approach (HFA) to include the effects of the screening and the Pauli blocking due to the FS.^{14,15} However, such a static treatment of the FS leads to a spurious bound state with respect to the Fermi energy, E_F , referred to in the following as the HFA bound state.¹⁹ This discrete state, with binding energy E_M , would appear at the energy $E_F - E_M$. Obviously, for $E_M < E_F$ (as in typical modulation-doped quantum wells), such a state cannot exist since it overlaps with the FS continuum, with which it interacts via the $e-h$ potential.^{14,15} The "unbinding" of this HFA bound state occurs via its interactions with the FS excitations,¹⁵ which are *not* taken into account in the HFA. Note that, in two-dimensional systems, a static FS allows for bound states even for arbitrarily small attractive interactions and therefore such an unbinding cannot arise from static screening or from Pauli blocking effects. This spurious bound state could be artificially merged with the continuum by introducing a dephasing time comparable to its binding energy. Such an approximation, however, neglects completely the interactions between the photoexcited

e - h pair and the FS excitations. A microscopic description of the unbinding of the HFA bound state presents a nontrivial problem due to the non-perturbative nature of the e - h correlations between the photoexcited hole and the FS excitations.¹⁵ Even within Green function techniques, this problem is rather involved because vertex correction diagrams with arbitrarily many crossed e - h interaction lines are as divergent as the ladder diagrams and should be treated on equal footing.²⁰ To perform such a task, one must sum up at least the parquet diagrams and address the three-body correlations between the photoexcited hole and a FS excitation.^{21,15} Therefore, alternative methods were developed for the case of linear absorption, based on Fermi's golden rule with many-electron eigenstates expressed in terms of Slater determinants.¹⁸ Such approaches become exact in the limit $m_e/m_h \ll 1$ (m_e and m_h are the electron and hole masses respectively) and describe quite accurately the FES lineshapes observed in typical modulation-doped quantum wells.^{18,22-24}

Another approach to the FES problem is based on the coupled cluster expansion (CCE).^{25,26} This general many-body technique provided exact results in the limit $m_e/m_h \ll 1$ ²⁷ and was used to treat the hole recoil correlations in one dimension.²⁸ In the latter case, an exact solution was obtained for $m_e = m_h$. The CCE has also been used to describe the e - e correlation effects²⁹. More importantly, however, this method is well-suited for describing correlations in non-equilibrium systems, where it retains the advantages of diagrammatic expansions without resorting to the Kadanoff-Baym ansatz or to the Markovian approximation.³⁰

Let us now briefly summarize recent experimental studies of dephasing and relaxation processes in modulation-doped quantum wells. Wang *et al.*³¹ performed pump-probe measurements under resonant excitation conditions and observed an incoherent redshift of the FES at positive time delays due to the incoherent bandgap renormalization. At room temperature, Knox *et al.*³² measured very fast e - e scattering times estimated ~ 10 fs, which implies extremely fast dephasing and relaxation. At low temperatures, Kim *et al.*³³ measured long dephasing times within the frequency range $\omega < E_F$ (the frequency domain of the FES), consistent with measurements in metals³⁴. This result is consistent with the Landau Fermi liquid theory³⁵ (which applies both to metals and doped-quantum wells due to the similar values of r_s) and points out that, unlike for the e - h correlations, the e - e scattering is suppressed within the frequency range of the FES. Furthermore, the above experiment suggests that the hole dephasing times are rather long. The above experimental results were interpreted within a two-level system approximation (which neglects all FES correlation effects) by introducing energy-dependent dephasing times obtained from the quasi-equilibrium e - e self-energies.³⁶ Note here that, unlike in undoped semiconductors, the relaxation of *real* photo-excited e - h pairs due to their interactions with the FS electrons³⁴ can obscure the role of the e - h correlations. However, these incoherent effects can be suppressed by tuning the pump frequency *below* the FES resonance and thus exciting only virtual carriers. In this case, coherent effects will dominate. Brener *et al.*^{37,38} performed such pump-probe measurements on doped QWs with well-below-resonance pump excitation and observed qualitatively different nonlinear optical dynamics for the FES as compared to excitons in undoped QWs. This suggests that the differences in the nature of the two resonances do manifest themselves in the transient changes of the optical properties.

In this paper, we develop a microscopic many-body theory for treating the coherent nonlinear optical response of the FES. In particular, we focus on the manifestations of the

non-perturbative e - h correlations (dynamical FS response) on the ultrafast time evolution of the pump-probe spectrum. In order to describe the dynamical FS response, we use a general formalism developed recently³⁹ (which we summarize in Appendix A). Within this approach, the transient pump-probe nonlinear absorption spectrum is mapped onto the linear absorption of a “pump-dressed” system, described by a time-dependent effective Hamiltonian. This allows us to treat the non-equilibrium e - h correlation effects non-perturbatively with the time-dependent version of the CCE. We mostly focus on negative time delays and off-resonant excitation conditions, in which case the coherent effects dominate.

In doped semiconductors, the pair-pair interactions, analogous to the exciton-exciton interactions in undoped semiconductors, are screened out, while the e - e scattering is suppressed for below-resonant excitation as dictated by Fermi Liquid theory. Instead, it is the e - h interactions between the photoexcited e - h pairs and the FS carriers that strongly affect the coherent ultrafast dynamics of the FES. An important difference from undoped semiconductors is that, due to its *gapless* pair excitation spectrum, a FS responds *unadiabatically* to time-dependent perturbations. In contrast, because of its finite Coulomb binding energy, an exciton can be polarized by the pump optical field without being ionized. A non-equilibrium treatment beyond the HFA is necessary in order to take into account the unadiabatic time-dependent *change* in the e - h pair-FS interactions and the e - h scattering processes induced by the ultrafast pump excitation. We study in detail the qualitative differences in the ultrafast dynamics with and without (HFA) the dynamical FS response and point out the important role of the e - h correlations in the coherent regime.

The outline of this paper is as follows. In Section II we summarize our formalism for the nonlinear optical response and in Section III we outline the basics of the CCE approach to correlations. In Section IV we obtain the time-dependent parameters of the effective semiconductor Hamiltonian and the effective optical transition matrix elements. In Section V we describe the effects of the optical excitation and the many-body correlations on the dynamics of the photoexcited e - h pair that determines the FES lineshape. In Section VI we present our results for the nonlinear absorption of the FES and its time-evolution, and discuss the role of the dynamical FS response. Section VII concludes the paper.

II. TRANSIENT NONLINEAR ABSORPTION SPECTRUM

We start by recapping the main points of our formalism³⁹ (see Appendix A). In the rotating frame,⁴⁰ the Hamiltonian describing this system is

$$H_{\text{tot}}(t) = H + H_p(t) + H_s(t). \quad (1)$$

The first term is the “bare” Hamiltonian,

$$H = \sum_{\mathbf{q}} \varepsilon_{\mathbf{q}}^v b_{-\mathbf{q}}^\dagger b_{-\mathbf{q}} + \sum_{\mathbf{q}} (\varepsilon_{\mathbf{q}}^c + \Omega) a_{\mathbf{q}}^\dagger a_{\mathbf{q}} + V_{ee} + V_{hh} + V_{eh}, \quad (2)$$

where $a_{\mathbf{q}}^\dagger$ is the creation operator of a conduction electron with energy $\varepsilon_{\mathbf{q}}^c$ and mass m_e , $b_{-\mathbf{q}}^\dagger$ is the creation operator of a valence hole with energy $\varepsilon_{\mathbf{q}}^v$ and mass m_h , V_{ee} , V_{eh} , and V_{hh} describe the e - e , e - h , and h - h interactions, respectively, and $\Omega = E_g + E_F(1 + m_e/m_h) - \omega_p$ is the detuning of the central frequency of the optical fields, ω_p , from the Fermi level, E_g being

the bandgap (we set $\hbar = 1$). The second and third terms describe the coupling of the pump optical field, $\mathcal{E}_p(t)e^{i\mathbf{k}_p \cdot \mathbf{r} - i\omega_p t}$, and the probe optical field, $\mathcal{E}_s(t)e^{i\mathbf{k}_s \cdot \mathbf{r} - i\omega_p(t-\tau)}$, respectively:

$$\begin{aligned} H_p(t) &= \mu \mathcal{E}_p(t) \left[e^{i\mathbf{k}_p \cdot \mathbf{r}} U^\dagger + \text{H.c.} \right], \\ H_s(t) &= \mu \mathcal{E}_s(t) \left[e^{i\mathbf{k}_s \cdot \mathbf{r} + i\omega_p \tau} U^\dagger + \text{H.c.} \right], \end{aligned} \quad (3)$$

where the pump amplitude $\mathcal{E}_p(t)$ is centered at time $t = 0$ and the probe amplitude $\mathcal{E}_s(t)$ is centered at the time delay $t = \tau$, μ is the interband transition matrix element, and

$$U^\dagger = \sum_{\mathbf{q}} a_{\mathbf{q}}^\dagger b_{-\mathbf{q}}^\dagger \quad (4)$$

is the optical transition operator. In Appendix B we clarify our convention for the time delay τ and relate it to the most commonly used conventions in pump/probe and four wave mixing (FWM) experiments.

In many experiments, the amplitude of the probe field is much smaller than that of the pump, $|\mathcal{E}_p(t)| \gg |\mathcal{E}_s(t)|$. In that case, as was shown in Ref. 39 (see Appendix A), the experimentally-measurable nonlinear optical polarization can be obtained in terms of the linear response functions of a “pump-dressed” semiconductor to a probe field (within $\chi^{(3)}$, this is true even for comparable pulse amplitudes). This “dressed” system is described by a time-dependent effective Hamiltonian $\tilde{H}(t)$, which is obtained by performing a time-dependent Schrieffer-Wolff/Van Vleck^{41,42} canonical transformation on the Hamiltonian $H + H_p(t)$. As we shall see in the next Section, in all the cases of interest, the effective Hamiltonian $\tilde{H}(t)$ has the same operator form as the bare Hamiltonian H , with the important difference that the band dispersions (effective masses) and interaction potentials are *time-dependent* through $\mathcal{E}_p(t)$. Thus, the calculation of the nonlinear absorption spectrum reduces to that of the linear absorption spectrum of the “pump-dressed” semiconductor with uncoupled “effective bands” — a great simplification that allows us to use straightforward generalizations of well established theoretical tools. It is important to note that, as was shown in Ref. 39 (see also Appendix A), such a “dressed semiconductor” approach is not restricted to monochromatic pulses and is valid for *any* pulse duration. In Appendix A, we show that the pump-probe nonlinear polarization has the following form :

$$P_{\mathbf{k}_s}(t) = -i\mu^2 e^{i\mathbf{k}_s \cdot \mathbf{r} - i\omega_p(t-\tau)} \int_{-\infty}^t dt' \mathcal{E}_s(t') \langle \Phi_0(t) | \tilde{U}(t) \mathcal{K}(t, t') \tilde{U}^\dagger(t') | \Phi_0(t') \rangle. \quad (5)$$

Here, $|\Phi_0(t)\rangle$ is the state evolved with $\tilde{H}(t)$ from the semiconductor ground state $|0\rangle$ of H , $\tilde{U}^\dagger(t)$ is the effective optical transition operator describing the probability amplitude for the photoexcitation of an e - h pair by the probe field in the presence of the pump excitation, and $\mathcal{K}(t, t')$ is the time-evolution operator satisfying the Schrödinger equation

$$i \frac{\partial}{\partial t} \mathcal{K}(t, t') = \tilde{H}(t) \mathcal{K}(t, t'). \quad (6)$$

The above equation describes the time evolution of a probe-photoexcited e - h pair in the presence of the pump excitation. The effective Hamiltonian and effective transition operator are given by (see Appendix A)

$$\tilde{H}(t) = H_0 - \frac{\mu}{2} \left(\mathcal{E}_p(t) [\hat{\mathcal{P}}(t), U^\dagger] + \text{H.c.} \right), \quad (7)$$

and

$$\tilde{U}^\dagger(t) = U^\dagger + \frac{1}{2} [\hat{\mathcal{P}}(t), [U^\dagger, \hat{\mathcal{P}}^\dagger(t)]] + \frac{1}{2} [\hat{\mathcal{P}}^\dagger(t), [U^\dagger, \hat{\mathcal{P}}(t)]], \quad (8)$$

where the operator $\hat{\mathcal{P}}^\dagger(t)$, which generates the canonical transformation, satisfies the equation

$$i \frac{\partial \hat{\mathcal{P}}^\dagger(t)}{\partial t} = [H, \hat{\mathcal{P}}^\dagger(t)] - \mu \mathcal{E}_p(t) U^\dagger, \quad (9)$$

with the initial condition $\hat{\mathcal{P}}^\dagger = 0$ before the pump arrives. Eqs. (7) and (8) include all the pump-induced corrections to $\tilde{U}^\dagger(t)$ and $\tilde{H}(t)$ up to the second order in the pump optical field and are valid when $(d_p/\Omega)^2 \lesssim 1$ (for off-resonant excitation) or $(d_p t_p)^2 \lesssim 1$ (for resonant excitation), where t_p is the pump duration.

It should be emphasized that, although Eq. (7) gives the effective Hamiltonian up to the second order in the pump field, $\mathcal{E}_p \mathcal{E}_p^*$, the polarization expression Eq. (5) describes the effects of \tilde{H} in *all* orders. For example, as we shall see in Section IV, the pump-induced term in \tilde{H} contains self-energy corrections to the electron/hole energies, which describe (among other effects) the resonance blueshift due to the ac-Stark effect. Although the *magnitude* of these self-energy corrections, calculated using Eq. (7), is quadratic in \mathcal{E}_p , the correct position of the resonance can only be obtained by evaluating the pump/probe polarization (5) nonperturbatively (beyond $\chi^{(3)}$), i.e., without resorting to the expansion of the time-evolution operator $\mathcal{K}(t, t')$ in the pump field. Importantly, the same is true when calculating the effects of the self-energy corrections on the e - h correlations. As we shall see in Section VI, such a nonperturbative (in the pump field) treatment of the non-linear response of the FES is crucial for the adequate description of the pump/probe spectrum at negative time delays. In Section V, we will describe the corresponding procedure, which accounts for the FS dynamical response. In contrast, the third-order polarization, $\chi^{(3)}$, can be simply obtained from Eq. (5) by expanding $\mathcal{K}(t, t')$ to the *first* order in the pump-induced term in \tilde{H} [second term in Eq. (7)]. We did not include in Eq. (5) the biexcitonic contribution (coming from the excitation of two e - h pairs by the pump *and* the probe pulses) since it vanishes for the negative time delays ($\tau < 0$) of interest here.³⁹

The important advantage of Eq. (5), as compared to the equations of motion for the polarization, comes from its similarity to the linear polarization that determines the linear absorption spectrum²⁰. This can be seen by setting $\mathcal{E}_p(t) = 0$ in the Eqs. (7) and (8), in which case the effective time-evolution and optical transition operators transform into their “bare” counterparts: $\mathcal{K}(t, t') \rightarrow e^{-iH(t-t')}$ and $\tilde{U}^\dagger(t) \rightarrow U^\dagger$. Moreover, like U^\dagger , the effective transition operator $\tilde{U}^\dagger(t)$ creates a single e - h pair, while, as we shall see below, the effective Hamiltonian $\tilde{H}(t)$ can be cast in a form similar to H . This allows one to interpret the Fourier transform of Eq. (5) as the linear absorption spectrum of a “pump-dressed” semiconductor with two uncoupled but time-dependent effective bands. This mapping simplifies significantly the calculation of the FES ultrafast nonlinear optical response by allowing a straightforward generalization of the CCE.

III. COUPLED-CLUSTER EXPANSION

In this Section, we show how the time-dependent CCE can be used to study the effects of the e - h correlations (dynamical FS response) on the time evolution of the e - h pair photoexcited by the probe. Our goal is to evaluate the many-body state $|\Psi(t)\rangle = \mathcal{K}(t, t')\tilde{U}^\dagger(t')|\Phi_0(t')\rangle$ that enters in Eq. (5). This state satisfies the Schrödinger equation

$$i\frac{\partial}{\partial t}|\Psi(t)\rangle = \tilde{H}(t)|\Psi(t)\rangle. \quad (10)$$

As already mentioned, $\tilde{H}(t)$ has the same form as the bare Hamiltonian H . This allows us to obtain $|\Psi(t)\rangle$ through a straightforward generalization of the linear absorption calculations^{26–28}. After eliminating the valence hole degrees of freedom,^{43,28} $|\Psi(t)\rangle$ is expressed in the CCE form

$$|\Psi(t)\rangle = e^{S(t)}|\Phi(t)\rangle, \quad (11)$$

where the time-dependent operator $S(t)$ creates FS-pairs and is given by

$$S(t) = \sum_{p>k_F, k<k_F} s(\mathbf{p}, \mathbf{k}, t)a_{\mathbf{p}}^\dagger a_{\mathbf{k}} + \sum_{p_1, p_2 > k_F, k_1, k_2 < k_F} s_2(\mathbf{p}_1, \mathbf{p}_2, \mathbf{k}_1, \mathbf{k}_2, t)a_{\mathbf{p}_1}^\dagger a_{\mathbf{p}_2}^\dagger a_{\mathbf{k}_2} a_{\mathbf{k}_1} + \dots, \quad (12)$$

while the state $|\Phi(t)\rangle$, discussed in Section V, describes the time evolution of the probe-induced e - h pair. In Eq. (12), the amplitude $s(\mathbf{p}, \mathbf{k}, t)$ describes the e - h correlations which, in particular, are responsible for the unbinding of the HFA bound state; the two-pair amplitude s_2 describes the e - e interaction effects at the RPA level and beyond. From a physical point of view, the operator $e^{S(t)}$ describes the readjustment of the FS density profile during the optical transition in response to the FS interactions with the photoexcited e - h pair.

Substituting Eq. (11) into the Schrödinger equation Eq. (10), multiplying by the operator $e^{-S(t)}$ from the lhs, and using the fact that $[S(t), S(t')] = [\dot{S}(t), S(t')] = 0$, we obtain

$$i\frac{\partial}{\partial t}|\Phi(t)\rangle + i\dot{S}(t)|\Phi(t)\rangle = e^{-S(t)}\tilde{H}(t)e^{S(t)}|\Phi(t)\rangle, \quad (13)$$

where the transformed Hamiltonian on the rhs can be expressed in terms of the commutator series (Baker-Campbell-Hausdorff expansion)

$$e^{-S(t)}\tilde{H}(t)e^{S(t)} = \tilde{H}(t) + [\tilde{H}(t), S(t)] + \frac{1}{2}[[H, S(t)], S(t)] + \dots \quad (14)$$

An important advantage of the CCE is that, due to the FS momentum restrictions in Eq. (12), the above series *terminates* after the first few terms (three for quartic interactions) and a closed-form expression of the transformed Hamiltonian (14) can be obtained in terms of $S(t)$. By requiring that all FS-pair creation processes are eliminated from the above equation, we obtain the CCE equations^{25,26} for $S(t)$. Before proceeding with such a calculation however, we derive in the next Section explicit expressions for $\tilde{H}(t)$ and $\tilde{U}(t)$.

IV. EFFECTIVE HAMILTONIAN AND OPTICAL TRANSITION OPERATOR

In this Section, we derive second-quantized expressions for the effective Hamiltonian $\tilde{H}(t)$ and optical transition operator $\tilde{U}(t)$. We start with Eqs. (7) and (8), which express $\tilde{H}(t)$ and $\tilde{U}(t)$ in terms of the canonical transformation operator $\hat{\mathcal{P}}^\dagger(t)$. The latter is given by Eq. (9), which includes the effects of the Coulomb interactions on the *pump* photoexcitation. It is important to realize that the effect of Coulomb e - h interactions on the pump and the probe photoexcitations is very different. For an adequate description of the FES, the e - h interactions should be taken into account *non-perturbatively* for the *probe*-photoexcited pair. Indeed, the nonlinear absorption spectrum at a given frequency ω close to the FES resonance is determined by the time-evolution for *long* times (of the order of the dephasing time T_2) of an e - h pair photoexcited by the *probe* at the energy ω .⁴⁴ Since the characteristic “ e - h interaction time” E_M^{-1} (inverse HFA bound state energy) that determines the nonexponential polarization decay is much shorter than the dephasing time, the long-time asymptotics of the response function (to the *probe*) depends non-perturbatively on the e - h interactions. In contrast, a short *pump* optical pulse excites a wavepacket of *continuum* e - h pair states (unlike in the discrete exciton case) with energy width $\sim t_p^{-1}$, which thus evolves during timescales comparable to the pulse duration t_p . Also, the corrections to the effective Hamiltonian are determined by the time evolution of the pump-induced carriers only up to times $\sim t_p$ (see Eq. (7)). Therefore, if the “ e - h interaction time” E_M^{-1} is larger than t_p , $t_p E_M \lesssim 1$, (i.e., if the pump pulse frequency width exceeds E_M), the e - h interactions can be treated perturbatively when describing the time-evolution of the *pump*-photoexcited pairs. This can also be shown explicitly for the third-order nonlinear polarization. In the general expression for $\chi^{(3)}$, all contributions that depend on the pump are integrated over the width of the pump pulse; therefore, any resonant enhancement of $\chi^{(3)}$ that depends on the pump frequency will be broadened out for sufficiently short pulses with frequency width that exceeds E_M . In other words, when deriving the pump-renormalized parameters, one can treat Coulomb interactions perturbatively if the above condition is fulfilled. In fact, the above situation is somewhat similar to the calculation of the linear absorption spectrum close to the indirect transition threshold, where perturbation theory can be used.^{15,21} Thus the above consideration applies even for long pulse durations provided that the detuning Ω exceeds E_M . This is certainly the case for the off-resonant excitation conditions considered in Section VI. However, in order to obtain the full absorption spectrum, the time-evolution of the *probe*-photoexcited pair with such effective Hamiltonian (with perturbatively calculated time-dependent parameters) should be treated *non-perturbatively*, as described in the following Section.

We now proceed with the derivation of the effective Hamiltonian. To lowest order in the interactions, $\hat{\mathcal{P}}^\dagger(t)$ can be presented as

$$\begin{aligned} \hat{\mathcal{P}}^\dagger(t) = & \sum_{\mathbf{q}} \mathcal{P}_{eh}(\mathbf{q}, t) a_{\mathbf{q}}^\dagger b_{-\mathbf{q}}^\dagger + \frac{1}{2} \sum_{\mathbf{p}, \mathbf{p}', \mathbf{k}} \mathcal{P}_{eh}^e(\mathbf{p}\mathbf{p}'; \mathbf{k}; t) b_{\mathbf{k}-\mathbf{p}-\mathbf{p}'}^\dagger a_{\mathbf{p}}^\dagger a_{\mathbf{p}}^\dagger a_{\mathbf{k}} \\ & + \frac{1}{2} \sum_{\mathbf{p}, \mathbf{p}', \mathbf{k}} \mathcal{P}_{eh}^h(\mathbf{p}\mathbf{p}'; \mathbf{k}; t) a_{\mathbf{p}+\mathbf{p}'-\mathbf{k}}^\dagger b_{-\mathbf{p}}^\dagger b_{-\mathbf{p}'}^\dagger b_{-\mathbf{k}}, \end{aligned} \quad (15)$$

where \mathcal{P}_{eh} is the probability amplitude for excitation of an e - h pair with zero momentum satisfying

$$i\frac{\partial}{\partial t}\mathcal{P}_{eh}(\mathbf{q}, t) = \left(\Omega + \varepsilon_{\mathbf{q}}^{(c)} + \varepsilon_{-\mathbf{q}}^{(v)} - i\Gamma\right)\mathcal{P}_{eh}(\mathbf{q}, t) - \mu\mathcal{E}_p(t) - \sum_{\mathbf{q}'} v(\mathbf{q} - \mathbf{q}')\mathcal{P}_{eh}(\mathbf{q}', t), \quad (16)$$

where $\Gamma = T_2^{-1}$ describes the dephasing due to processes not included in the Hamiltonian H (e.g., due to phonons). In Eq. (15),

$$\mathcal{P}_{eh}^e(\mathbf{p}\mathbf{p}'; \mathbf{k}; t) = i\int_{-\infty}^t dt' e^{-i(t-t')\left(\Omega + \varepsilon_{\mathbf{p}}^c + \varepsilon_{\mathbf{p}'}^c - \varepsilon_{\mathbf{k}}^c + \varepsilon_{\mathbf{p}+\mathbf{p}'-\mathbf{k}}^v - i\Gamma\right)} \times \\ \{v(\mathbf{p} - \mathbf{k})[\mathcal{P}_{eh}(\mathbf{p}', t') - \mathcal{P}_{eh}(\mathbf{p} + \mathbf{p}' - \mathbf{k}, t')] - (\mathbf{p} \leftrightarrow \mathbf{p}')\} \quad (17)$$

describes the scattering of the photoexcited e - h pair with an electron, and

$$\mathcal{P}_{eh}^h(\mathbf{p}\mathbf{p}'; \mathbf{k}; t) = -i\int_{-\infty}^t dt' e^{-i(t-t')\left(\Omega + \varepsilon_{\mathbf{p}+\mathbf{p}'-\mathbf{k}}^c + \varepsilon_{\mathbf{p}'}^v + \varepsilon_{\mathbf{p}}^v - \varepsilon_{\mathbf{k}}^v - i\Gamma\right)} \times \\ \{v(\mathbf{p} - \mathbf{k})[\mathcal{P}_{eh}(\mathbf{p}', t') - \mathcal{P}_{eh}(\mathbf{p} + \mathbf{p}' - \mathbf{k}, t')] - (\mathbf{p} \leftrightarrow \mathbf{p}')\} \quad (18)$$

describes the scattering of the photoexcited e - h pair with a hole. The above expressions describe in the lowest order in the screened interaction⁴⁵ $v(\mathbf{p} - \mathbf{k})$ the coherent pump-induced processes, the effects of the Hartree-Fock pair-pair and pair-FS interactions, and the dynamical FS response to the *pump* photoexcitation.

By substituting Eq. (15) into Eq. (8), we obtain the following expression for the effective optical transition operator:

$$\tilde{U}^\dagger(t)|\Phi_0(t)\rangle = \sum_{p>k_F} M_{\mathbf{p}}(t)a_{\mathbf{p}}^\dagger b_{-\mathbf{p}}^\dagger|0\rangle + \frac{1}{4}\sum_{p,p'>k_F, k<k_F} M_{\mathbf{p}\mathbf{p}'\mathbf{k}}(t)a_{\mathbf{p}}^\dagger a_{\mathbf{p}'}^\dagger b_{\mathbf{k}-\mathbf{p}-\mathbf{p}'}^\dagger a_{\mathbf{k}}|0\rangle, \quad (19)$$

where the effective matrix element $M_{\mathbf{p}}(t)$ includes corrections due to phase space filling and Hartree-Fock interactions, and $M_{\mathbf{p}\mathbf{p}'\mathbf{k}}(t)$ is the probability amplitude for indirect optical transitions¹⁵ induced by the pump optical field, which contribute to the pump-probe polarization in the second order in the interactions. The explicit expressions for $M_{\mathbf{p}}(t)$ and $M_{\mathbf{p}\mathbf{p}'\mathbf{k}}(t)$ are given in Appendix C.

We turn now to the effective Hamiltonian $\tilde{H}(t)$. After substituting Eq. (15) into Eq. (7) we obtain that

$$\tilde{H}(t) = \sum_{\mathbf{q}} \varepsilon_{\mathbf{q}}^v(t)b_{-\mathbf{q}}^\dagger b_{-\mathbf{q}} + \sum_{\mathbf{q}} \varepsilon_{\mathbf{q}}^c(t)a_{\mathbf{q}}^\dagger a_{\mathbf{q}} + V_{eh}(t) + V_{ee}(t), \quad (20)$$

where

$$\varepsilon_{\mathbf{q}}^c(t) = \varepsilon_{\mathbf{q}}^c + \mu\mathcal{E}_p(t)\text{Re}\left[\mathcal{P}_{eh}(\mathbf{q}, t) - \sum_{\mathbf{q}'} \mathcal{P}_{eh}^e(\mathbf{q}\mathbf{q}'; \mathbf{q}; t)\right] \quad (21)$$

is the effective conduction electron energy;

$$\varepsilon_{\mathbf{q}}^v(t) = E_g + \varepsilon_{\mathbf{q}}^v + \mu\mathcal{E}_p(t)\text{Re}\left[\mathcal{P}_{eh}(\mathbf{q}, t) - \sum_{\mathbf{q}'} \mathcal{P}_{eh}^h(\mathbf{q}\mathbf{q}'; \mathbf{q}; t)\right], \quad (22)$$

is the effective valence hole energy;

$$V_{eh}(t) = - \sum_{\mathbf{k}\mathbf{k}'\mathbf{q}} v_{eh}(\mathbf{q}; \mathbf{k}\mathbf{k}'; t) a_{\mathbf{k}+\mathbf{q}}^\dagger a_{\mathbf{k}} b_{-\mathbf{k}'-\mathbf{q}}^\dagger b_{-\mathbf{k}'}, \quad (23)$$

is the effective e - h interaction; and

$$V_{ee}(t) = \frac{1}{2} \sum_{\mathbf{k}\mathbf{k}'\mathbf{q}} v_{ee}(\mathbf{q}; \mathbf{k}\mathbf{k}'; t) a_{\mathbf{k}+\mathbf{q}}^\dagger a_{\mathbf{k}'-\mathbf{q}}^\dagger a_{\mathbf{k}'} a_{\mathbf{k}}, \quad (24)$$

is the effective e - e interaction. The explicit expressions for $v_{eh}(\mathbf{q}; \mathbf{k}\mathbf{k}'; t)$ and $v_{ee}(\mathbf{q}; \mathbf{k}\mathbf{k}'; t)$ are given in Appendix C. As can be seen, $\tilde{H}(t)$ has the same operator form as the bare Hamiltonian H . However, both the effective band dispersions and the effective interaction potentials are now *dependent on time*. Note here that the above pump-induced renormalizations only last for the pulse duration t_p . As discussed above, they are therefore perturbative in the screened interactions for $t_p E_M \lesssim 1$ or for $\Omega > E_M$.

Let us first discuss the effect of the pump-induced self-energy corrections to the conduction and valence band energies, given by the last terms in Eqs. (21) and (22). The dispersion of the effective band is shown in Fig. 1. As can be seen, the pump pulse leads to a bandgap increase as well as a change in the momentum dependence (band dispersion) that last *as long as the pump pulse*. The magnitude of the bandgap increase is of the order of $(\mu\mathcal{E}_p)^2/\Omega$ (for off-resonant excitation) and $(\mu\mathcal{E}_p)^2 t_p$ (for resonant excitation) and leads to, e.g., the ac-Stark blueshift. As we shall see, for pulse duration shorter than the dephasing time, it also leads to bleaching and gain right below the onset of absorption, analogous to the case of excitons or two-level systems.^{2,3} It should be emphasized that these are *coherent* effects that should not be confused with the incoherent bandgap redshift due to the e - e interactions among real photoexcited carriers.³¹ Note also that the above bandgap renormalization is induced by the *transverse* EM-field of the laser, as compared to the usual bandgap renormalization due to a *longitudinal* EM-field, i.e., Coulomb screening. The change in the band dispersion, whose relative magnitude is of the order of $(\mu\mathcal{E}_p/\Omega)^2$ (for off-resonant excitation) or $(\mu\mathcal{E}_p t_p)^2$ (for resonant excitation), can be viewed as an increase in the effective density of states and, to the first approximation, in the effective mass. This is important in doped semiconductors because, as we shall see later, it leads to a time-dependent enhancement of the e - h interactions and scattering processes with the FS electrons.

The effective Hamiltonian $\tilde{H}(t)$ also includes pump-induced corrections in the effective interaction potentials, determined by the pair-pair and pair-FS interactions during the pump photoexcitation. By expanding Eqs. (C3) and (C4) for carrier energies close to the Fermi surface using Eqs. (17) and (18), one can show that these corrections vanish at the Fermi surface; for the typical FS excitation energies $\Delta\varepsilon \sim E_M$ that contribute to the FES, their order of magnitude is $(\mu\mathcal{E}_p \Delta\varepsilon/\Omega^2)^2$ (for off-resonant excitation) or $(\mu\mathcal{E}_p \Delta\varepsilon t_p^2)^2$ (for resonant excitation). Thus the corrections to the interaction potentials are suppressed for below-resonant excitation by a factor of $(E_M/\Omega)^2$, or for short pulses by a factor of $(E_M t_p)^2$, as compared to the self-energy corrections. Such a suppression is due to the Pauli blocking effect and the screening, which leads to the vanishing of the pump-induced corrections to the interaction potentials at the Fermi surface. Similarly, the pump-induced indirect optical transition matrix elements $M_{\mathbf{p}\mathbf{p}'\mathbf{k}}(t)$ are suppressed by the same factor as compared to the direct transition matrix element $M_{\mathbf{p}}(t)$ [first term in Eq. (19)], while they contribute to the pump-probe polarization only in the second order in the screened interactions. Therefore,

in the doped case, the screened Coulomb interaction leads to subdominant parameter renormalizations to the effective Hamiltonian $\tilde{H}(t)$ and transition operator $\tilde{U}^\dagger(t)$ for sufficiently short pump pulses or for off-resonant excitation. In the following Section, we study the e - h dynamics caused by the pump-induced self-energies and direct transition matrix elements which lead to the strongest nonlinearities in the case of below-resonant or short pulse excitation.

V. ELECTRON-HOLE DYNAMICS

In this Section, we derive the final formulae for the nonlinear pump-probe polarization of the interacting system by applying the CCE to the effective Hamiltonian $\tilde{H}(t)$ in order to treat the dynamical FS response. The CCE equation Eq. (13) contains the operator $S(t)$ described by a hierarchy of coupled equations for the amplitudes s, s_2, \dots , defined by Eq. (12). In the coherent case of interest here, the e - e scattering effects are suppressed, and the nonlinear absorption spectrum is dominated by the e - h interactions. This allows us to use the dephasing time approximation for treating the probe-induced e - e scattering processes^{36,22-24}, in which case the above hierarchy terminates after s . Importantly, the e - h correlations (dynamical FS response) are still treated non-perturbatively, since they are determined by s .²⁶⁻²⁸ Then all FS-pair creation processes can be eliminated explicitly from the rhs of Eq. (13), leading to the following nonlinear differential equation for the one-FS-pair scattering amplitude,²⁶⁻²⁸ $s(\mathbf{p}, \mathbf{k}, t)$:

$$i \frac{\partial s(\mathbf{p}, \mathbf{k}, t)}{\partial t} - [\varepsilon_{\mathbf{p}}^c(t) - \varepsilon_{\mathbf{k}}^c(t)] s(\mathbf{p}, \mathbf{k}, t) = V \left[1 + \sum_{\mathbf{p}' > k_F} s(\mathbf{p}', \mathbf{k}, t) \right] \left[1 - \sum_{\mathbf{k}' < k_F} s(\mathbf{p}, \mathbf{k}', t) \right]. \quad (25)$$

The e - h scattering processes described by the above equation are sketched in Fig. 2a. Here V is the s -wave component¹⁴ of the screened interaction⁴⁵, approximated for simplicity by its value at the Fermi energy.^{15,22,23} This neglects plasmon effects, which are however small within the frequency range of the FES.^{46,36} Although this approximation is standard for the linear absorption case, its justification for the transient spectra requires more attention. Indeed, the characteristic time for screening buildup is of the order Ω_p^{-1} , where Ω_p is the typical plasma frequency corresponding to the FS.^{47,48,44,46} This time is however shorter than the typical pump duration ~ 100 fs and dephasing time (which is of the order of ps near the Fermi energy),^{31,33} so the Coulomb interactions can be considered screened also for the nonlinear absorption case. In Eq. (25), we neglected the hole recoil energy contribution to the excitation energy²⁸ since $\varepsilon_{k_F}^v(t) - \varepsilon_0^v(t) \lesssim E_M$ due to a sufficiently heavy hole mass.¹⁵ Note that, by increasing the hole effective mass, the pump-induced hole self-energy, Eq. (22), reduces the hole recoil energy and thus the corresponding broadening.¹⁵ In real samples, the relaxation of the momentum conservation condition due to the disorder will also suppress the hole recoil broadening effects.

From Eq. (13) we then easily obtain the following expression for $|\Phi(t)\rangle$:

$$|\Phi(t)\rangle = \sum_{p > k_F} \Phi_{\mathbf{p}}(t, t') a_{\mathbf{p}}^\dagger b^\dagger |0\rangle, \quad (26)$$

where b^\dagger is the creation operator of the zero-momentum hole state and the e - h pair wavefunction $\Phi_{\mathbf{p}}(t, t')$ satisfies the ‘‘Wannier-like’’ equation of motion,

$$i\frac{\partial\Phi_{\mathbf{p}}(t,t')}{\partial t} = \left[\Omega + \varepsilon_{\mathbf{p}}^c(t) + \varepsilon_{-\mathbf{p}}^v(t) - \varepsilon_A(t) - i\Gamma_{\mathbf{p}}\right] \Phi_{\mathbf{p}}(t,t') - \tilde{V}(\mathbf{p},t) \sum_{p'>k_F} \Phi_{\mathbf{p}'}(t,t'), \quad (27)$$

where

$$\tilde{V}(\mathbf{p},t) = V \left[1 - \sum_{k'<k_F} s(\mathbf{p},\mathbf{k}',t) \right], \quad (28)$$

is the effective e - h potential whose *time- and momentum-dependence* is determined by the response of the FS electrons to their interactions with the probe-induced e - h pair (vertex corrections) [sketched schematically in Fig. 2(b), responsible for the unbinding of the HFA bound state],

$$\varepsilon_A(t) = V \sum_{k'<k_F} \left[1 + \sum_{p'>k_F} s(\mathbf{p}',\mathbf{k}',t) \right] \quad (29)$$

is the self-energy due to the sudden appearance of the photoexcited hole, which leads to non-exponential polarization decay [described by $\text{Im} \varepsilon_A(t)$] due to the Anderson orthogonality catastrophe¹⁶ and a dynamical resonance redshift [described by $\text{Re} \varepsilon_A(t)$], and $\Gamma_{\mathbf{p}}$ describes all additional dephasing processes (due to e - e interactions, hole recoil, and phonons). Eq. (27) should be solved with the initial condition $\Phi_{\mathbf{p}}(t',t') = M_{\mathbf{p}}(t')$, where $M_{\mathbf{p}}(t')$ is defined by Eq. (19).

It is worth stressing here the analogy between Eqs. (26) and (27) and the corresponding problem in undoped semiconductors. Indeed, Eq. (26) is the direct analog of an exciton state, whereas again Eq. (27) is very similar to a Wannier equation. However, Eqs. (25) and (27) include the effects of the interactions between the probe-photoexcited e - h pair and the FS-excitations, and the wavefunction $\Phi_{\mathbf{p}}(t,t')$ describes the propagation of the photoexcited pair “dressed” by the FS excitations. Such a “dressing” is due to the dynamical FS response, which leads to the dynamical screening of the effective e - h interaction Eq. (28). The time-dependence of the latter is determined by the FS scattering amplitude $s(\mathbf{p},\mathbf{k},t)$ and is affected by the pump excitation as described by Eq. (25). One can easily verify that by setting $s(\mathbf{p},\mathbf{k},t) = 0$ in Eq. (27), we recover the results of the Hartree-Fock (ladder diagram, static FS¹⁵) approximation. If one neglects the nonlinear (quadratic) term in Eq. (25), one recovers the three-body (Fadeev) equations.^{15,49} Note that the coupled equations for $\Phi_{\mathbf{p}}(t,t')$ and $s(\mathbf{p},\mathbf{k},t)$, obtained by neglecting the multipair excitations in Eq. (12), can be extended to include the hole recoil-induced corrections.²⁸

Using Eqs. (11), (12), and (26), we now can express the pump-probe polarization Eq. (5) in terms of the e - h wavefunction Φ and the effective transition matrix element $M_{\mathbf{p}}$. Assuming, for simplicity, a delta-function probe pulse centered at time delay τ , $\mathcal{E}_s(t) = \mathcal{E}_s\delta(t - \tau)$, we obtain a simple final expression ($t > \tau$):

$$P_{\mathbf{k}_s}(t) = -i\mu^2\mathcal{E}_s e^{i\mathbf{k}_s \cdot \mathbf{r} - i\omega_p(t-\tau)} \sum_{p>k_F} M_{\mathbf{p}}(t)\Phi_{\mathbf{p}}(t,\tau). \quad (30)$$

Eq. (30) expresses the pump-probe polarization in terms of two physically distinct contributions. First is the effective transition matrix element $M_{\mathbf{p}}(t)$, which includes the effects of pair-pair and pair-FS interactions and Phase space filling effects due to the pump-induced

carriers present during the probe photoexcitation. Second is the wavefunction $\Phi_{\mathbf{p}}(t)$ of the e - h pair photoexcited by the probe, whose time dependence, determined by Eqs. (27) and (25), describes the formation of the absorption resonance. Despite the formal similarities, there are two important differences between the doped and the undoped cases. First, in the doped case, the time evolution of the e - h wavefunction $\Phi_{\mathbf{p}}(t)$ is strongly affected by the interplay between the e - h correlations and the pump-induced transient changes in the bandgap and band dispersion relations. As we shall see later, this can be viewed as an excitation-induced dephasing. Second, unlike in the undoped case,³⁹ the pump-induced corrections in the effective matrix element $M_{\mathbf{p}}(t)$ are perturbative in the screened interactions if the pump detuning or the pump frequency width exceed the Coulomb energy E_M . In the next Section, we demonstrate the role of each of these effects both analytically (for CW excitation) and numerically (for short pulses).

VI. PUMP-PROBE DYNAMICS

A. Monochromatic Excitation

In this subsection, we analyze the FES pump-probe spectrum in the case of monochromatic excitation. For monochromatic pump, the theory developed in the previous Sections applies for pump detunings larger than the characteristic Coulomb energy, $\Omega \gtrsim E_M$. Close to the Fermi edge, the linear absorption spectrum of the FES can be approximately described with the analytic expression^{15,18}

$$\alpha(\omega) \propto \mathcal{N} \left(\frac{E_F}{\omega} \right)^\beta, \quad (31)$$

where \mathcal{N} is the density of states, ω is the optical frequency measured from the Fermi edge, and $\beta = 2\delta/\pi - (\delta/\pi)^2$ is the FES exponent, where $\delta \sim \tan^{-1}(\pi g)$ is the s -wave phaseshift of the screened e - h potential evaluated at E_F , and $g = \mathcal{N}V$ is the dimensionless parameter characterizing the scattering strength. The monochromatic pump excitation leads to a resonance blueshift, originating from the shift in the effective band energies (see Fig. 1), and to a bleaching mainly due to the Pauli blocking which reduces the effective transition matrix element (analogous to the dressed atom picture⁴²). More importantly, however, the pump-induced change in the band dispersion increases the density of states \mathcal{N} close to the Fermi surface and thus also increases both the e - h scattering strength g and the phaseshift δ . This, in turn, leads to an increase in the FES exponent β that determines the resonance width and lineshape. In contrast, in the case of a bound excitonic state of dimensionality D and Bohr radius a_B , the resonance width remains unchanged, while the oscillator strength, $\propto a_B^{-D}$, increases by a factor $\sim (1 + D \Delta m)$, where Δm is the pump-induced change in the effective mass⁵⁰. Such an optically-induced enhancement of the exciton strength competes with the bleaching due to the Pauli blocking and exciton-exciton interactions. This results in an almost rigid exciton blueshift, consistent with experiment^{51,52} and previous theoretical results⁵³.

However, in the case of a FES resonance, the pump-induced change in the exponent β leads to a stronger oscillator strength enhancement than for a bound exciton state. Obviously, such an enhancement cannot be described perturbatively, i.e., with an expansion in

terms of the optical field, since the corresponding corrections to the absorption spectrum diverge logarithmically at the Fermi edge. As can be seen from Eq. (31), the effect of the pump on the FES can be thought of as an excitation-induced dephasing that affects the *frequency dependence* of the resonance; again, this is in contrast to the case of the exciton. In the time domain, this also implies a memory structure related to the response-time of the FS-excitations. Therefore, the qualitative differences between the nonlinear optical response of the FES and the exciton originate from the fact that an exciton is a discrete bound state, while the FES is a *continuum* many-body resonance. The FS responds *unadiabatically* to the pump-induced change in the density of states via an *increase* in the *e-h* scattering of *low-energy* pair excitations. Such scattering processes, which determine the response of the Fermi sea to the hole potential in the course of the optical excitation, are responsible for the unbinding and broadening of the HFA bound state.⁴⁴ Therefore, the pump field changes the broadening and dephasing effects even for below-resonant photoexcitation. On the other hand, due to the finite Coulomb binding energy of the exciton, the pump optical field can polarize such a bound state and change its Bohr radius without ionizing it. In the next subsection, we study the above effects in the case of short pulse excitation.

B. Short-pulse Excitation

We now present our results for the nonlinear absorption of the FES in the case of short pulse excitation. The results were obtained by solving numerically the differential equations (27) and (25), using the Runge-Kutta method, for Gaussian pulses with duration $t_p = 2.0E_F^{-1}$. We only considered negative time delays and focussed on below-resonant pump excitation in order to suppress the incoherent effects due to the *e-e* scattering of real pump-induced carrier populations with the FS. Under such excitation conditions, the *coherent* effects in which we are interested dominate, and the Coulomb-induced corrections to the effective parameters, discussed in Section IV, are perturbative. Our goal is to study the role of the dynamical FS response (*e-h* correlations) on the pump-probe dynamics. For this reason we compare the results of our theory to those of the HFA, obtained by setting $s(\mathbf{p}, \mathbf{k}, t) = 0$ in Eq. (27). As mentioned above, in the latter case, the (spurious) HFA bound state does not interact with the FS pair excitations, even though it can merge with the continuum when one introduces a very short dephasing time.

In Fig. 3, we compare the linear absorption lineshape (in the absence of pump, $\mathcal{E}_p(t) = 0$) of the FES to the HFA (without the dynamical FS response). We use the parameter values $g = 0.4$ and $\Gamma = 0.1E_F$, which were previously used to fit the experimental spectra in modulation doped quantum wells.^{22,18} For better visibility, we shifted the curves in order to compare their lineshapes. The linear absorption FES lineshape is consistent with that obtained in Refs. 18 and 27. On the other hand, the HFA spectrum is characterized by the coexistence of the bound state and a continuum contribution due to the fact that, in 2D, a bound state exists even for an arbitrary weak attractive potential. We note that if one limits oneself to linear absorption, it is possible to artificially shorten the dephasing time $T_2 = \Gamma^{-1}$, mainly determined by the hole recoil effects, by taking $\Gamma \simeq E_M$. Then the spurious discrete state and the continuum merge, and the discrepancy between the two linear absorption lineshapes decreases. This trick has been used for phenomenological fits of linear absorption experimental data.¹⁷ Below we show, however, that in the nonlinear

absorption case, the differences in the transient spectra are significant so that the processes beyond HFA can be observed experimentally.

Let us turn to the time evolution of the pump–probe spectra. In Fig. 4 we show the nonlinear absorption spectra calculated by including the dynamical FS response (Fig. 4(a)) and within the HFA (Fig. 4(b)) at a short time delay $\tau = -t_p/2$. The main features of the spectrum are a pump–induced resonance bleaching, blueshift, and gain right below the onset of absorption. For off–resonant pump, these transient effects vanish for positive time delays after the pump is gone, and persist for negative time delays shorter than the dephasing time $T_2 = \Gamma^{-1}$. Similar features were also obtained for different values of the pump amplitude, duration, and detuning. They are mainly due to the broadening induced by the transient renormalization of the energy band dispersion [Eqs. (21) and (22)] when its duration $\sim t_p$ is shorter than the dephasing time (analogous to excitons and two–level systems^{2,3}).

We now turn to the role of the e – h correlations. In Fig. 5 we compare the differential transmission spectrum calculated by including the dynamical FES response or within the HFA for long and short negative time delays. Note that, in pump/probe spectroscopy, the experimentally measured differential transmission is

$$DST(\omega, \tau) = \frac{\Delta T_s(\omega, \tau)}{T_0(\omega)} = \frac{T_s(\mathcal{E}_p) - T_s(\mathcal{E}_p = 0)}{T_s(\mathcal{E}_p = 0)}, \quad (32)$$

where $T_s(\mathcal{E}_p)$ is the transmission coefficient in the probe direction in the presence of the pump field \mathcal{E}_p . In the weak signal regime, it reproduces the changes in the probe absorption coefficient $\alpha(\omega, \tau)$: $DST(\omega, \tau) \propto -\Delta\alpha(\omega, \tau)$. Fig. 5(a) shows the results obtained for a long time delay, $\tau = -1.5T_2 = -15.0E_F^{-1}$, in which case frequency domain oscillations are observed. These oscillations are similar to those seen in undoped semiconductors and two–level systems; however, their amplitude in the FES case is reduced. On the other hand, as shown in Fig. 5(b), for time delays comparable to the pulse duration, $\tau = -0.1T_2 = -t_p/2 = -1.0E_F^{-1}$, the main features are a blueshift and bleaching. In this case the e – h correlations lead to a substantially larger width and asymmetric lineshape of the differential transmission spectrum. This comes from the different response of the FES to the pump–induced dispersion renormalizations when the e – h correlations are accounted for. This is more clearly seen in Fig. 6(a), where we plot the magnitude of the resonance decrease, evaluated at the peak frequency, as a function of τ . We use, of course, the same values of the parameters in the two calculations and yet we find that the bleaching of the FES peak is substantially stronger when the dynamical FS response is included than in the HFA case. Note that for $|\tau| \sim \Gamma^{-1}$ the FES resonance is actually enhanced by the pump, as can be seen more clearly in Fig. 7. The time dependence of the resonance bleaching is strikingly different in the two cases. In the HFA case, $|DST(\omega, \tau)|$ evaluated at the instantaneous peak frequency decays over a time scale $|\tau| \sim \Gamma^{-1}$, i.e. during the dephasing time. This is similar to results obtained for a two–level system with the same effective parameters. On the other hand, the decay of $|DST(\omega, \tau)|$ at the peak frequency is much faster when we take into account the e – h correlations. Note that the above results were obtained for off–resonant excitation. Under resonant conditions, we find that a spectral hole is produced. In Fig. 8 we compare the resonance blueshifts, evaluated at the peak frequency, as a function of τ . Again, a larger blueshift is predicted when the dynamical FS response is included. This suggests that in the experiment of Ref. 37, where similar blueshifts were observed in two

quantum well samples (one modulation doped with a FES and one undoped sample with a 2D-exciton) the effective parameters were larger in the latter case, due to the absence of screening and exciton–exciton interaction effects.

In order to gain qualitative understanding of the role of the e – h correlations, let us for a moment neglect the momentum dependence of the pump–renormalization of the band dispersion and the phase space filling effects and consider the bleaching caused by a rigid semiconductor band shift $\Delta E_g(t)$, obtained from the pump–induced self–energies, Eqs. (21) and (22), evaluated at the bottom of the band (note that $\Delta E_g(t)$ lasts for the duration of pulse). Within this model, the pump excitation has no effect on the e – h scattering amplitude $s(\mathbf{p}, \mathbf{k}, t)$ [see Eq. (25)]. It is thus convenient to factorize the effects of the rigid band shift on the e – h wavefunction $\Phi_{\mathbf{p}}(t, t')$:

$$\Phi_{\mathbf{p}}(t, t') = e^{-i \int_{t'}^t \Delta E_g(t'') dt''} \tilde{\Phi}_{\mathbf{p}}(t, t'). \quad (33)$$

This relation is general and defines $\tilde{\Phi}_{\mathbf{p}}(t, t')$, which does *not* depend on $\Delta E_g(t)$. In the special case of a rigid shift, $\tilde{\Phi}_{\mathbf{p}}(t, t')$ coincides with $\Phi_{\mathbf{p}}^0(t - t')$ describing the propagation of the probe–photoexcited e – h pair in the *absence* of the pump pulse. By substituting into Eq. (33) the long–time asymptotic expression⁴⁴ $\tilde{\Phi}_{\mathbf{p}}(t, t') = \Phi_{\mathbf{p}}^0(t - t') \propto [i(t - t')E_F]^{\beta-1}$ that gives the linear absorption spectrum of the FES at $\omega \simeq E_F$, and substituting the resulting $\Phi_{\mathbf{p}}(t, t')$ into Eq. (30), we obtain a simple analytic expression for the effect of a pump–induced rigid band shift on the nonlinear absorption spectrum:

$$\alpha(\omega) \propto \text{Re} \int_{\tau}^{\infty} dt e^{i(\omega+i\Gamma)(t-\tau)-i \int_{\tau}^t \Delta E_g(t') dt'} [i(t - \tau)E_F]^{\beta-1}. \quad (34)$$

For $\Delta E_g(t) = 0$ one, of course, recovers the linear FES absorption in the vicinity of the Fermi edge.⁴⁴ For $\beta = 0$, Eq. (34) gives the absorption of the non–interacting continuum.

The physics of the FES can be seen from Eq. (34). For $\beta = 1$, this gives a discrete Lorentzian peak corresponding to the HFA bound state. However, during the optical transition, the e – h pair interacts with the FS electrons, leading to the and the readjustment of the FS density profile via the scattering of FS pairs. This results in the broadening of the discrete HFA bound state, which is governed by the time evolution of the FS. Such time evolution is unadiabatic due to the low–energy FS pairs, which leads to the characteristic power–law time dependence of the broadening factor in Eq. (34). The interaction with the FS–pairs determines the exponent, $0 \leq \beta \leq 1$, of the latter, which leads to a non–Lorentzian lineshape in the frequency domain and a non–exponential decay in the time domain. A detailed discussion of the above physics and the analogy to phonon sidebands and collision broadening may be found in Ref. 44. Here it is essential to use the CCE in order to calculate the spectrum at *all* frequencies (and not just asymptotically close to E_F as with Eq. (34)) and, most importantly, to describe the non–equilibrium FS and e – h pair response to the time–dependent increase in the effective mass/density of states, not included in Eq. (34).

The resonance bleaching obtained from Eq. (34) as a function of τ , is shown in Fig. 6(b) for $\beta = 0.6$, corresponding to the value of the parameters used in Fig. 6(a) ($g = 0.4$), together with the HFA result ($\beta = 1$). Comparing Figs. 6(a) and (b), one can see that the rigid band shift approximation qualitatively accounts for the dynamics, but that there are strong discrepancies (see vertical scales), whose origin is discussed below. Both the magnitude and the time–dependence of the bleaching depends critically on the value of β ,

which characterizes the interaction of the photoexcited e - h pair with the FS excitations. Because of such coupling, many polarization components are excited in the case of the continuum FES resonance, and it is their interference that governs the dynamics of the pump/probe signal. Such interference is also responsible for the resonance enhancement and differential transmission oscillations at $\tau < 0$ shown in Figs. 5 and 7. As β increases the interference effects are suppressed because the energy width of the continuum states contributing to the FES narrows. In fact, this energy width is directly related to that of the linear absorption resonance. This is clearly seen in Fig. 9 where we show the effect of increasing g on the dynamics of the bleaching. It becomes more bound-state-like as, with increasing g , the FES resonance becomes narrower. On the other hand, in the HFA case, the decay rate is $\sim T_2 = \Gamma^{-1}$, i. e. it is independent on g , when E_M becomes smaller than Γ , while for $E_M \simeq \Gamma$, the contribution of the continuum states produce a faster decay.

Although the transient rigid band shift approximation, Eq. (34), explains some of the features of the dynamics of the bleaching, it strongly overestimates its magnitude. This is because Eq. (34) neglects the response of the many-body system to the pump-induced renormalization of the band's dispersion, neglected in Eq. (34). Such a transient change in the dispersion, which can be viewed as an increase in the density of states/effective mass for the duration of the pump, is important because it results in an enhancement of the e - h scattering. For example, in the case of monochromatic excitation, this leads to the change in the exponent β of the broadening prefactor in the integrand of Eq. (34), discussed in the previous subsection. For the short-pulse case, it is not possible to describe analytically the effect of the pump on the e - h scattering processes, due to the non-equilibrium unadiabatic FS response. The latter can be described with the numerical solution of Eqs. (25) and (27), which is presented in Figs. 10 and 11 and discussed below.

In order to show the role of the pump-induced renormalization of the band dispersion in the presence of the dynamical FS response, we plot in Fig. 10 the function

$$F(\omega, \tau) = \text{Im} \sum_{p > k_F} \tilde{\Phi}_{\mathbf{p}}(\omega, \tau) \quad (35)$$

where $\tilde{\Phi}_{\mathbf{p}}(\omega, \tau)$ is the Fourier transform of $\tilde{\Phi}_{\mathbf{p}}(t, \tau)$ defined by Eq. (33). Note that, in the presence of the band dispersion renormalization, the wave-function $\tilde{\Phi}_{\mathbf{p}}$ (which is independent of $\Delta E_g(t)$) no longer coincides with $\Phi_{\mathbf{p}}^0$ as in Eq. (34). As can be seen in Fig. 10(a), when the e - h correlations are taken into account, the pump-induced redistribution of oscillator strength between the states of the continuum that contribute to the resonance manifests itself as a dynamical redshift. This shift opposes the rigid band blueshift $\Delta E_g(t)$ (when the latter is included). At the same time, the resonance strength is enhanced significantly. The latter effect originates from the interplay between the transient increase in the effective mass/density of states of the photoexcited e - h pair and the “dressing” of this pair with the FS excitations [described by the effective potential $\tilde{V}(\mathbf{p}, t)$ in Eq. (27)]. In contrast, such an oscillator strength enhancement is suppressed in the HFA (which neglects the e - h correlations), as seen in Fig. 10(b), in which case the main feature is the redshift of the resonance due to the pump-induced increase of the binding energy E_M coming from the transient increase in the effective mass [see Fig. 10(b)].

In Fig. 11 we show the effect of the renormalization of the band dispersion on the non-linear absorption spectrum. The optically-induced increase in the e - h interactions enhances

significantly the strength of the FES and compensates part of the bleaching induced by the rigid band shift. A smaller enhancement is also seen in the HFA, where the pump-induced increase in the binding energy E_M competes with the effects of the bandgap renormalization.

VII. CONCLUSIONS

In summary, we developed a theory for the ultrafast nonlinear optical response of the FES. We focussed on coherent effects, which dominate the pump-probe spectra during negative time delays and off-resonant excitation conditions. We demonstrated that the dynamical FS response leads to qualitatively different coherent dynamics of the FES as compared to the Hartree-Fock approximation. In particular, in the former case, the time evolution of the resonance bleaching is governed by the dephasing time, while in the former case polarization interference effects dominate. This results in faster FES dynamics (which depends on the strength of the screened $e-h$ potential) as well as an apparent resonance enhancement during negative time delays. Such dynamical features should be observable in ultrafast pump/probe experiments. Using a simple model, we showed that the different dynamics of the FES and Hartree-Fock treatment can be attributed to the non-Lorentzian broadening of the HFA bound state due to its interactions with the gapless FS excitations, a process which is, of course, beyond the dephasing time approximation. In addition, we showed that the pump excitation directly affects the strength of the $e-h$ scattering processes, which changes the frequency dependence of the resonance. The latter can be thought of as an excitation-induced dephasing effect that leads to a transient enhancement of the FES. Our results indicate that ultrafast spectroscopy provides a powerful tool to study the role of correlations in the nonlinear response of a Fermi liquid to the optical excitation during time scales shorter than the dephasing times. The dynamical features discussed above can also be used as an experimental signal to probe the crossover from FES to exciton bound state (exciton Mott transition) as a function of the FS density.

ACKNOWLEDGMENTS

This work was supported by the NSF Grant No. ECS-9703453, by a grant from the HITACHI Advanced Research Laboratory, and in part by the Office of Naval Research grant No. N00014-96-1-1042. The work of D.S.C. was supported by the Director, Office of Energy Research, Office of Basic Energy Sciences, Division of Material Sciences of the U.S. Department of Energy, under Contract No. DE-AC03-76SF00098.

APPENDIX A:

In this appendix we briefly outline our formalism.³⁹ The pump-probe signal is determined by the polarization,

$$P(t) = \mu e^{-i\omega_p t} \langle \Psi(t) | U | \Psi(t) \rangle, \quad (\text{A1})$$

where the state $|\Psi(t)\rangle$ satisfies the time-dependent Schrödinger equation,

$$\left[i \frac{\partial}{\partial t} - H_{tot}(t) \right] |\Psi(t)\rangle = \left[i \frac{\partial}{\partial t} - H - H_p(t) - H_s(t) \right] |\Psi(t)\rangle = 0, \quad (\text{A2})$$

with the Hamiltonians H and $H_{p,s}(t)$, given by Eqs. (2)–(3). The Hilbert space of the bare semiconductor, i.e. in the absence of optical fields, consists of disconnected subspaces $\zeta\{\nu_{eh}\}$ which are labeled by the number of (interband) e - h pairs, ν_{eh} . The corresponding bare Hamiltonian, H , conserves the number of e - h pairs in each band separately and in the $\zeta\{\nu_{eh}\}$ -basis has a block-diagonal form. The Hamiltonians $H_{p,s}(t)$ couple the different subspaces $\zeta\{\nu_{eh}\}$ by causing interband transitions.

In the description of pump/probe experiments, we are interested only in the polarization component propagating along the probe direction \mathbf{k}_s . For a weak probe, the nonlinear signal then arises from the linear response of the pump/bare-semiconductor coupled system, described by the time-dependent Hamiltonian $H + H_p(t)$, to the probe-induced perturbation $H_s(t)$. Within $\chi^{(3)}$, the above is true even for comparable pump and probe amplitudes. However, since, in contrast to H , the Hamiltonian $H + H_p(t)$ does not conserve the number of carriers in each band separately, the calculation of the linear response function is not practical. Therefore, we seek to replace $H + H_p(t)$ by an effective Hamiltonian $\tilde{H}(t)$ that *does* conserve the number of e - h pairs in each of its Hilbert subspaces (i.e., is “block-diagonal”). As derived in Ref. 39, this can be accomplished in any given order in the pump field $\mathcal{E}_p(t)$ and for any pulse duration by using a time-dependent Schrieffer-Wolff/Van Vleck canonical transformation^{41,42}. Here it is sufficient to “block-diagonalize” the Hamiltonian $H + H_p(t)$ up to the second order in $\mathcal{E}_p(t)$. The transformation that achieves this has the form $e^{-\hat{T}_2} e^{-\hat{T}_1} [H + H_p(t)] e^{\hat{T}_1} e^{\hat{T}_2}$, where the anti-Hermitian operators $\hat{T}_1(t)$ and $\hat{T}_2(t)$ create/annihilate one and two e - h pairs, respectively.

We proceed with the first step and eliminate the single-pair pump-induced transitions in the time-dependent Schrödinger equation of the pump/bare-semiconductor system,

$$\left[i \frac{\partial}{\partial t} - H - H_p(t) \right] |\Psi(t)\rangle = 0. \quad (\text{A3})$$

This is achieved by substituting $|\Psi(t)\rangle = e^{\hat{T}_1(t)} |\chi(t)\rangle$ and acting with the operator $e^{-\hat{T}_1(t)}$ on the lhs of Eq. (A3),

$$e^{-\hat{T}_1(t)} \left[i \frac{\partial}{\partial t} - H \right] e^{\hat{T}_1(t)} |\chi(t)\rangle = e^{-\hat{T}_1(t)} [H_p(t)] e^{\hat{T}_1(t)} |\chi(t)\rangle. \quad (\text{A4})$$

The anti-Hermitian operator $\hat{T}_1(t)$ has a decomposition

$$\hat{T}_1(t) = \hat{\mathcal{P}}(t) e^{-i\mathbf{k}_p \cdot \mathbf{r}} - \hat{\mathcal{P}}^\dagger(t) e^{i\mathbf{k}_p \cdot \mathbf{r}}, \quad (\text{A5})$$

where $\hat{\mathcal{P}}^\dagger(t)$ and $\hat{\mathcal{P}}(t)$ create and annihilate single e - h pairs, respectively. The effective Hamiltonian can be found from the condition that the terms describing single-pair interband transitions cancel each other in Eq. (A4). In Ref. 39, it was shown that the multiple commutators of $\hat{\mathcal{P}}(t)$ with its time derivatives can be eliminated from Eq. (A4) to all orders. By expanding Eq. (A4) and neglecting third or higher order terms in $\hat{\mathcal{P}}$, we obtain the following equation:

$$i\frac{\partial\hat{\mathcal{P}}^\dagger(t)}{\partial t} = [H, \hat{\mathcal{P}}^\dagger(t)] - \mu\mathcal{E}_p(t)U^\dagger, \quad (\text{A6})$$

with initial condition $\hat{\mathcal{P}}^\dagger(-\infty) = 0$. The formal solution is

$$\hat{\mathcal{P}}^\dagger(t) = i\mu \int_{-\infty}^t dt' \mathcal{E}_p(t') e^{-iH(t-t')} U^\dagger e^{iH(t-t')}. \quad (\text{A7})$$

Note that, since the Hamiltonian H conserves the number of e - h pairs and the optical transition operator U^\dagger creates a single e - h pair, $\hat{\mathcal{P}}^\dagger(t)$ also creates a single e - h pair. Furthermore, since both H and U^\dagger conserve momentum, so does $\hat{\mathcal{P}}^\dagger(t)$. Eq. (A4) then takes the form

$$\left[i\frac{\partial}{\partial t} - \tilde{H}(t) \right] |\chi(t)\rangle = -\frac{\mu}{2} [\mathcal{E}_p(t)e^{2i\mathbf{k}_p\mathbf{r}} [U^\dagger, \hat{\mathcal{P}}^\dagger(t)] + \text{H.c.}] |\chi(t)\rangle, \quad (\text{A8})$$

where

$$\tilde{H}(t) = H - \frac{\mu}{2} (\mathcal{E}_p(t) [\hat{\mathcal{P}}(t), U^\dagger] + \text{H.c.}) \quad (\text{A9})$$

is the sought time-dependent effective Hamiltonian that conserves the number of e - h pairs and $\hat{\mathcal{P}}^\dagger(t)$ is given by Eq. (A6). Note that, since $\hat{\mathcal{P}}^\dagger(t)$ is linear in the pump field \mathcal{E}_p , the pump-induced term in $\tilde{H}(t)$ [second term in Eq. (A9)] is quadratic ($\propto \mathcal{E}_p\mathcal{E}_p^*$). The rhs of Eq. (A8) describes the pump-induced two-pair transitions. These can be eliminated as well by performing a second canonical transformation, $|\chi(t)\rangle = e^{\hat{T}_2(t)}|\Phi(t)\rangle$. Following the same procedure, we use the anti-Hermiticity of $\hat{T}_2(t)$ to decompose it as

$$\hat{T}_2(t) = \hat{\mathcal{P}}_2^\dagger(t)e^{-2i\mathbf{k}_p\mathbf{r}} - \mathcal{P}_2^\dagger(t)e^{2i\mathbf{k}_p\mathbf{r}}, \quad (\text{A10})$$

where $\mathcal{P}_2^\dagger(t)$ and $\hat{\mathcal{P}}_2(t)$ create and annihilate two e - h pairs, respectively. Substituting the above expression for $|\chi(t)\rangle$ into Eq. (A8) and requiring that all two-pair transitions cancel out, we obtain the following equation for $\mathcal{P}_2^\dagger(t)$,

$$i\frac{\partial\mathcal{P}_2^\dagger(t)}{\partial t} = [\tilde{H}(t), \mathcal{P}_2^\dagger(t)] - \frac{\mu}{2} \mathcal{E}_p(t)[\hat{\mathcal{P}}^\dagger(t), U^\dagger]. \quad (\text{A11})$$

Note that $\hat{\mathcal{P}}_2^\dagger(t)$ only affects the pump/probe polarization via higher order (\mathcal{E}_p^4) corrections, which are neglected here. However, it does determine the four-wave-mixing (FWM) polarization (see below).

To obtain the condition of validity of this approach, it is useful to write down a formal solution (A7) of Eq. (A6) in the basis of the N -hole many-body eigenstates, $|\alpha N\rangle$, with energies $E_{\alpha N}$, of the Hamiltonian H . Here the index α labels all the other quantum numbers, so that $N=0$ corresponds to the semiconductor ground state $|0\rangle$, $|\alpha 1\rangle$ denotes the one-pair states (exciton eigenstates in the undoped case, with α labeling both bound and scattering states), $|\alpha 2\rangle$ denotes the two-pair (biexciton in the undoped case) eigenstates, etc. In this basis, the solution of Eq. (A6) can be written as

$$\frac{\langle\beta N + 1|\hat{\mathcal{P}}^\dagger(t)|\alpha N\rangle}{\langle\beta N + 1|U^\dagger|\alpha N\rangle} = i\mu \int_{-\infty}^t dt' \mathcal{E}_p(t') e^{-i(t-t')(\Omega + \Delta E_{\alpha\beta}^N)} e^{-\Gamma(t-t')}, \quad (\text{A12})$$

where we separated out the detuning Ω and denoted $\Delta E_{\alpha\beta}^N = E_{\beta N+1} - E_{\alpha N}$. It can be seen that for resonant excitation (small Ω) the rhs of Eq. (A12) is of the order of $\mu\mathcal{E}_p t_p$. Thus, for short pulses, this parameter justifies the expansion in terms of the optical fields. For off-resonant excitation, this expansion is valid for any pulse duration provided that $\mu\mathcal{E}_p/\Omega \lesssim 1$. Similar conditions can be obtained for the two-pair transition described by $\hat{\mathcal{P}}_2$.

The nonlinear polarization Eq. (A1) can now be expressed in terms of the linear response to the probe field:

$$P(t) = \mu e^{-i\omega_p t} \langle \Psi(t) | U | \Psi(t) \rangle = \mu e^{-i\omega_p t} \langle \Phi(t) | U_T(t) | \Phi(t) \rangle, \quad (\text{A13})$$

where, in the first order in $\mathcal{E}_s(t)$, the state $|\Phi(t)\rangle$ is given by

$$|\Phi(t)\rangle = |\Phi_0(t)\rangle - i\mu \int_{-\infty}^t dt' \mathcal{K}(t, t') \left[\mathcal{E}_s(t') e^{i\mathbf{k}_s \cdot \mathbf{r} + i\omega_p \tau} U_T^\dagger(t') + \text{H.c.} \right] |\Phi_0(t')\rangle. \quad (\text{A14})$$

Here $\mathcal{K}(t, t')$ is the time-evolution operator satisfying

$$i \frac{\partial}{\partial t} \mathcal{K}(t, t') = \tilde{H}(t) \mathcal{K}(t, t'), \quad (\text{A15})$$

and $U_T^\dagger(t) = e^{-\hat{T}_2(t)} e^{-\hat{T}_1(t)} U^\dagger e^{\hat{T}_1(t)} e^{\hat{T}_2(t)}$ is the (transformed) optical transition operator. In Eq. (A14), $|\Phi_0(t)\rangle = \mathcal{K}(t, -\infty) |0\rangle$ is the time-evolved ground state $|0\rangle$; since $\tilde{H}(t)$ conserves the number of e - h pairs, $|\Phi_0(t)\rangle$ contains no interband e - h pairs (in undoped semiconductors, it coincides with the ground state, $|\Phi_0(t)\rangle = |0\rangle$). From Eqs. (A14) and (A13), the polarization $P(t)$ takes the form

$$\begin{aligned} P(t) = & -i\mu^2 e^{-i\omega_p t} \int_{-\infty}^t dt' \\ & \times \left[\langle \Phi_0(t) | U_T(t) \mathcal{K}(t, t') \left[\mathcal{E}_s(t') e^{i\mathbf{k}_s \cdot \mathbf{r} + i\omega_p \tau} U_T^\dagger(t') + \mathcal{E}_s^*(t') e^{-i\mathbf{k}_s \cdot \mathbf{r} - i\omega_p \tau} U_T(t') \right] | \Phi_0(t') \rangle \right. \\ & \left. - \langle \Phi_0(t') | \left[\mathcal{E}_s(t') e^{i\mathbf{k}_s \cdot \mathbf{r} + i\omega_p \tau} U_T^\dagger(t') + \mathcal{E}_s^*(t') e^{-i\mathbf{k}_s \cdot \mathbf{r} - i\omega_p \tau} U_T(t') \right] \mathcal{K}(t', t) U_T(t) | \Phi_0(t) \rangle \right]. \quad (\text{A16}) \end{aligned}$$

The above expression for the *total* polarization contains contributions propagating in various directions. To obtain the polarization propagating in a specific direction, one has to expand the effective-transition operator $U_T(t)$ in terms of \hat{T}_1 and \hat{T}_2 . Using Eqs. (A5) and (A10) and keeping only terms contributing to pump/probe and FWM polarizations, we obtain³⁹

$$U_T^\dagger(t) = U_1^\dagger(t) + U_2^\dagger(t) e^{i\mathbf{k}_p \cdot \mathbf{r}} + U_{FWM}(t) e^{-2i\mathbf{k}_p \cdot \mathbf{r}} + \dots, \quad (\text{A17})$$

where (to lowest order in the pump field)

$$\begin{aligned} U_1^\dagger(t) &= U^\dagger + \frac{1}{2} [\hat{\mathcal{P}}(t), [U^\dagger, \hat{\mathcal{P}}^\dagger(t)]] + \frac{1}{2} [\hat{\mathcal{P}}^\dagger(t), [U^\dagger, \hat{\mathcal{P}}(t)]], \\ U_2^\dagger(t) &= [\hat{\mathcal{P}}^\dagger(t), U^\dagger], \\ U_{FWM}^\dagger(t) &= \frac{1}{2} [[U, \hat{\mathcal{P}}^\dagger(t)], \hat{\mathcal{P}}^\dagger(t)] - [U, \hat{\mathcal{P}}_2^\dagger(t)]. \quad (\text{A18}) \end{aligned}$$

Here operators $U_1^\dagger(t) \equiv \tilde{U}(t)$ and $U_{FWM}^\dagger(t)$ create one e - h pair, while $U_2^\dagger(t)$ creates two e - h pairs (note that U_{FWM} in Eq. (A18) annihilates an e - h pair).

Pump/probe polarization

In order to extract the pump/probe polarization from Eq. (A16), one should retain only terms that are proportional to $e^{i\mathbf{k}_s \cdot \mathbf{r}}$. Substituting Eqs. (A17) into Eq. (A16), we obtain $P_{\mathbf{k}_s}(t) = P_{\mathbf{k}_s}^{(1)}(t) + P_{\mathbf{k}_s}^{(2)}(t)$, where

$$P_{\mathbf{k}_s}^{(1)}(t) = -i\mu^2 e^{i\mathbf{k}_s \cdot \mathbf{r} - i\omega_p(t-\tau)} \int_{-\infty}^t dt' \mathcal{E}_s(t') \langle \Phi_0(t) | \tilde{U}(t) \mathcal{K}(t, t') \tilde{U}^\dagger(t') | \Phi_0(t') \rangle, \quad (\text{A19})$$

and

$$P_{\mathbf{k}_s}^{(2)}(t) = -i\mu^2 e^{i\mathbf{k}_s \cdot \mathbf{r} - i\omega_p(t-\tau)} \int_{-\infty}^t dt' \mathcal{E}_s(t') \langle \Phi_0(t) | U_2(t) \mathcal{K}(t, t') U_2^\dagger(t') | \Phi_0(t') \rangle. \quad (\text{A20})$$

Note that the above formulae apply to both undoped and doped semiconductors.

Eqs. (A19)–(A20) express the nonlinear pump/probe polarization in terms of the linear response to the probe field of a system described by the time-dependent effective Hamiltonian (A9). Such a form for the nonlinear response allows one to distinguish between two physically distinct contributions to the optical nonlinearities. Assuming that a short probe pulse arrives at $t = \tau$, consider the first term, Eq. (A19), which gives the single-pair (exciton for undoped case) contribution to the pump/probe polarization. At negative time delays, $\tau < 0$, the probe excites an e - h pair, described by state $\tilde{U}^\dagger(\tau) | \Phi_0(\tau) \rangle \simeq U^\dagger | 0 \rangle$; since the probe arrives before the pump, the effective transition operator coincides with the “bare” one [see Eqs. (A18) and (A7)]. The first contribution to the optical nonlinearities comes from the effective Hamiltonian, $\tilde{H}(t)$, governing the propagation of that interacting e - h pair in the interval (τ, t) via the time-evolution operator $\mathcal{K}(t, \tau)$. Note that since the pump pulse arrives at $t = 0$, for $|\tau| \gg \Gamma^{-1}$, the negative time-delay signal vanishes. At $t > 0$, the e - h pair (exciton in the undoped case) “feels” the effect of the pump via mainly the transient bandgap shift, leading, e.g., to ac-Stark effect, and the change in the band dispersions (increase in effective mass/density of states), leading to enhanced e - h scattering (exciton binding energy in the undoped case). Note that $\tilde{H}(t)$ also contains a contribution coming from the interactions between probe- and pump-excited e - h pairs, which are however perturbative in the doped case for short pulses or off-resonant excitation [see Section IV] and lead to subdominant corrections. Importantly, the response of the system to the optically-induced corrections in $\tilde{H}(t)$ takes into account *all* orders in the pump field, which is necessary for the adequate description, e.g., of the ac-Stark effect and the pump-induced changes in the e - h correlations. Indeed, although the pump-induced term in Eq. (A9) is quadratic in \mathcal{E}_p , the time-evolution of the interacting e - h pair is described without expanding $\mathcal{K}(t, \tau)$ in the pump field. On the other hand, the third-order polarization ($\chi^{(3)}$) can be obtained by expanding $\mathcal{K}(t, \tau)$ to the lowest order. The second contribution to the optical nonlinearities comes from the matrix element of the final state, $\langle \Phi_0(t) | \tilde{U}(t)$ in Eq. (A19). The latter, given by Eq. (A18), contains the lowest order (quadratic) pump-induced terms which describe the Pauli blocking, pair-pair, and pair-FS interaction effects (exciton-exciton interactions in the undoped case³⁹). Note that the matrix element of the *initial* state contributes for positive time delays, i.e., if the probe arrives after the pump pulse. In this case, however, the pump-induced term in the effective Hamiltonian (A9) vanishes (since it lasts only for the duration of the pulse) so that for positive $\tau > t_p$ the pump/probe signal is determined

by the matrix elements rather than by $\tilde{H}(t)$. If the probe arrives during the interaction of the system with the pump pulse ($\tau \sim t_p$), both the effective Hamiltonian and the matrix elements contribute to the polarization. In this case, there is also a biexcitonic contribution [given by Eq. (A20)] coming from a simultaneous excitation of two e - h pairs by the pump *and* the probe. However, such a biexciton state does *not* contribute to negative ($\tau < 0$) time delays. As can be seen from the above discussion, our theory separates out a number of contributions that play a different role for different time delays and excitation conditions.

FWM polarization

By extracting from Eq. (A16) all the terms propagating in the the FWM direction, $2\mathbf{k}_p - \mathbf{k}_s$, we obtain³⁹ (for delta-function probe $\mathcal{E}_s(t) = \mathcal{E}_s\delta(t - \tau)$)

$$P_{FWM}(t) = -i\mu^2 e^{i(2\mathbf{k}_p - \mathbf{k}_s) \cdot \mathbf{r} - i\omega_p(t+\tau)} \mathcal{E}_s^* \left[\langle \Phi_0(t) | U\mathcal{K}(t, \tau) U_{FWM}^\dagger(\tau) | \Phi_0(\tau) \rangle - (t \leftrightarrow \tau) \right], \quad (\text{A21})$$

where the FWM transition operator $U_{FWM}^\dagger(t)$ is given by Eq. (A18) and $t \geq \tau$. It is convenient to express $U_{FWM}^\dagger(t)$ in terms of the ‘‘irreducible’’ two-pair operator $W^\dagger(t) = \frac{1}{2}\hat{\mathcal{P}}^{\dagger 2} - \hat{\mathcal{P}}_2^\dagger$, satisfying

$$i\frac{\partial W^\dagger(t)}{\partial t} = [\tilde{H}(t), W^\dagger(t)] - \mu\mathcal{E}_p(t)U^\dagger\hat{\mathcal{P}}^\dagger(t). \quad (\text{A22})$$

In terms of $W^\dagger(t)$, the state $U_{FWM}^\dagger(t)|\Phi_0(t)\rangle$ in Eq. (A21) can be presented as a sum of two- and one-pair contributions:

$$U_{FWM}^\dagger(t)|\Phi_0(t)\rangle = UW^\dagger(t)|\Phi_0(t)\rangle - \hat{\mathcal{P}}^\dagger(t)U\hat{\mathcal{P}}^\dagger(t)|\Phi_0(t)\rangle. \quad (\text{A23})$$

The operator $W^\dagger(t)$, being quadratic in the pump field ($\propto \mathcal{E}_p^2$), describes the simultaneous excitation of two interacting e - h pairs by the pump pulse and includes the two-photon coherence effects (biexciton and exciton-exciton scattering effects in the undoped case). The corresponding state, $W^\dagger(t)|\Phi_0(t)\rangle$, satisfies the four-particle (two-exciton for the undoped case) Schrödinger-like equation with a source term [coming from the second term in the rhs of Eq. (A22)] and can be expressed in terms of the two-exciton Green function³⁹. The first term in Eq. (A23) is responsible for the (interaction-induced) finite FWM signal when the probe arrives after the pump.⁵ The second term in Eq. (A23), after being substituted into Eq. (A21), describes the diffraction of the pump field on the grating $\mathbf{k}_p - \mathbf{k}_s$ due to the interference of the pump and probe electric fields, and contributes to the Pauli blocking and single-exciton effects. Note that, similarly to the pump/probe polarization, Eq. (A21) gives contributions to the FWM polarization in all orders in the pump field; in this case, however, the third-order polarization $\chi^{(3)}$ can be obtained by simply neglecting the difference between $\tilde{H}(t)$ and H in the time-evolution operator $\mathcal{K}(t, \tau)$ and in the equation for $W^\dagger(t)$ because $U_{FWM}^\dagger(t)$ is already quadratic in the pump field. For $\chi^{(3)}$, the connection between our formalism and that of Axt and Stahl^{11,5} can be established by considering the matrix elements of the operator $W^\dagger(t)$ between two e - h pair states.³⁹

APPENDIX B:

In this appendix we clarify our convention for the time delay τ and relate it to the most commonly used conventions in Pump/probe and Four Wave Mixing experiments. In the generic experimental configuration two laser pulses $E_1(t)e^{i\mathbf{k}_1 \cdot \mathbf{r} - i\omega(t-t_1)}$, and $E_2(t)e^{i\mathbf{k}_2 \cdot \mathbf{r} - i\omega(t-t_2)}$, respectively centered at time $t = t_1$ and $t = t_2$ are incident on a sample. Let us define Δt as,

$$\Delta t = t_1 - t_2 \quad (\text{B1})$$

and consider a FWM experiment where the signal is measured in the direction $2\mathbf{k}_2 - \mathbf{k}_1$. Then for a two-level-atom, the signal vanishes for $\Delta t < 0$, while for $\Delta t > 0$ its amplitude, which decays with time as e^{-t/T_2} , is determined by the Pauli blocking. In a system with Coulomb interactions (such as a semiconductor) a FWM signal is observed both for $\Delta t < 0$ and $\Delta t > 0$. The $\Delta t < 0$ signal is entirely due to the Coulomb interaction.

In pump/probe experiments, one usually chooses one pulse (the ‘‘pump’’) to have an amplitude E_p much larger than that of the other pulse (the ‘‘probe’’), E_s . As discussed in the text, a weak probe measures the linear response of the system (bare or dressed by the pump). If we choose that $E_p = E_2$, the pump induces coherent and incoherent populations when it arrives in the sample *before* the probe i.e. for $t_2 < t_1$. This is usually defined as ‘‘positive’’ time delay $\tau = t_2 - t_1 > 0$ in the pump/probe literature. Note that $\tau = -\Delta t$, i.e., the ‘‘regular’’ sequence in pump/probe experiments is the *reverse* of that of FWM experiments. For $\tau < 0$, the origin of the pump/probe signal is that the probe creates a linear polarization in the sample which lasts for time $\sim T_2 = \Gamma^{-1}$ and, consequently, is scattered by polarization excited by the pump field. The signal observed for $\tau < 0$ is therefore due to coherent effects.

In FWM experiments, there is no restriction on the magnitude of the two incident fields E_2 and E_1 , which are often chosen to have amplitudes of the same order. Note however that, at the $\chi^{(3)}$ level, the FWM and pump–probe polarizations are linear in the $E_1(t)$ field and thus the above linear response calculation applies even for comparable pump and probe amplitudes.

APPENDIX C:

In this Appendix we present the explicit expressions for the renormalized transition matrix elements in the presence of the pump excitation. The direct transition matrix element is given by

$$\begin{aligned} M_{\mathbf{p}}(t) = & 1 - |\mathcal{P}_{eh}(\mathbf{p}, t)|^2 + \left[\mathcal{P}_{eh}^*(\mathbf{p}, t) \sum_{k' < k_F} \mathcal{P}_{eh}^e(\mathbf{p}\mathbf{k}'; \mathbf{k}'; t) + \text{H.c.} \right] \\ & - \frac{1}{2} \sum_{p' > k_F} \mathcal{P}_{eh}^*(\mathbf{p}', t) \left[\mathcal{P}_{eh}^e(\mathbf{p}'\mathbf{p}; \mathbf{p}'; t) - \mathcal{P}_{eh}^h(\mathbf{p}'\mathbf{p}; \mathbf{p}'; t) - \mathcal{P}_{eh}^h(\mathbf{p}'\mathbf{p}; \mathbf{p}; t) + \mathcal{P}_{eh}^e(\mathbf{p}'\mathbf{p}; \mathbf{p}; t) \right] \\ & + \frac{1}{2} \sum_{p' > k_F} \left[\mathcal{P}_{eh}(\mathbf{p}, t) + \mathcal{P}_{eh}(\mathbf{p}', t) \right] \left[\mathcal{P}_{eh}^e(\mathbf{p}\mathbf{p}'; \mathbf{p}; t) + \mathcal{P}_{eh}^h(\mathbf{p}\mathbf{p}'; \mathbf{p}; t) \right]^*. \end{aligned} \quad (\text{C1})$$

The first term on the rhs of the above equation describes the phase space filling contribution, while the rest of the terms are due to the mean field pair–pair and pair–FS interactions.

The pump–induced indirect transition matrix element is given by

$$\begin{aligned}
M_{\mathbf{p}\mathbf{p}'\mathbf{k}}(t) = & \left[\mathcal{P}_{eh}(\mathbf{k}, t) - \mathcal{P}_{eh}(\mathbf{p} + \mathbf{p}' - \mathbf{k}, t) \right]^* \mathcal{P}_{eh}^e(\mathbf{p}\mathbf{p}'; \mathbf{k}; t) \\
& - \left[\mathcal{P}_{eh}(\mathbf{p}, t) + \mathcal{P}_{eh}(\mathbf{p}', t) \right]^* \left[\mathcal{P}_{eh}^e(\mathbf{p}\mathbf{p}'; \mathbf{p}; t) + \mathcal{P}_{eh}^{h*}(\mathbf{p}\mathbf{p}'; \mathbf{p} + \mathbf{p}' - \mathbf{k}; t) \right] \\
& + \mathcal{P}_{eh}(\mathbf{p} + \mathbf{p}' - \mathbf{k}, t) \left[\mathcal{P}_{eh}^e(\mathbf{k}, \mathbf{p} + \mathbf{p}' - \mathbf{k}; \mathbf{p}'; t) - \mathcal{P}_{eh}^e(\mathbf{k}, \mathbf{p} + \mathbf{p}' - \mathbf{k}; \mathbf{p}; t) \right]^* \\
& + \mathcal{P}_{eh}^*(\mathbf{k}, t) \left[\mathcal{P}_{eh}^h(\mathbf{k}, \mathbf{p} + \mathbf{p}' - \mathbf{k}; \mathbf{p}'; t) + \mathcal{P}_{eh}^e(\mathbf{p}, \mathbf{p}'; \mathbf{k}; t) \right. \\
& \left. - \mathcal{P}_{eh}^e(\mathbf{p}, \mathbf{p}'; \mathbf{p} + \mathbf{p}' - \mathbf{k}; t) - \mathcal{P}_{eh}^h(\mathbf{k}, \mathbf{p} + \mathbf{p}' - \mathbf{k}; \mathbf{p}; t) \right] \\
& + \mathcal{P}_{eh}(\mathbf{p}, t) \mathcal{P}_{eh}^{e*}(\mathbf{k}, \mathbf{p} + \mathbf{p}' - \mathbf{k}; \mathbf{p}'; t) - \mathcal{P}_{eh}(\mathbf{p}', t) \mathcal{P}_{eh}^{e*}(\mathbf{k}, \mathbf{p} + \mathbf{p}' - \mathbf{k}; \mathbf{p}; t). \quad (\text{C2})
\end{aligned}$$

The effective e – h potential is given by

$$\begin{aligned}
v_{eh}(\mathbf{q}; \mathbf{k}\mathbf{k}'; t) = & v(\mathbf{q}) - \frac{\mu}{2} \mathcal{E}_p(t) \left[\mathcal{P}_{eh}^e(\mathbf{k} + \mathbf{q}, \mathbf{k}'; \mathbf{k}' + \mathbf{q}; t) + \mathcal{P}_{eh}^h(\mathbf{k}, \mathbf{k}' + \mathbf{q}; \mathbf{k}'; t) \right] \\
& - \frac{\mu}{2} \mathcal{E}_p(t) \left[\mathcal{P}_{eh}^e(\mathbf{k}, \mathbf{k}' + \mathbf{q}; \mathbf{k}'; t) + \mathcal{P}_{eh}^h(\mathbf{k} + \mathbf{q}, \mathbf{k}'; \mathbf{k}' + \mathbf{q}; t) \right]^*, \quad (\text{C3})
\end{aligned}$$

and the effective e – e potential is given by

$$\begin{aligned}
v_{ee}(\mathbf{q}; \mathbf{k}\mathbf{k}'; t) = & v(\mathbf{q}) + \frac{\mu}{4} \mathcal{E}_p(t) \left[\mathcal{P}_{eh}^e(\mathbf{k} + \mathbf{q}, \mathbf{k}' - \mathbf{q}; \mathbf{k}'; t) - \mathcal{P}_{eh}^e(\mathbf{k} + \mathbf{q}, \mathbf{k}' - \mathbf{q}; \mathbf{k}; t) \right] \\
& + \frac{\mu}{4} \mathcal{E}_p(t) \left[\mathcal{P}_{eh}^e(\mathbf{k}, \mathbf{k}'; \mathbf{k}' - \mathbf{q}; t) - \mathcal{P}_{eh}^e(\mathbf{k}, \mathbf{k}'; \mathbf{k} + \mathbf{q}; t) \right]^*. \quad (\text{C4})
\end{aligned}$$

REFERENCES

- ¹ For recent reviews see D. S. Chemla, *Ultrafast Transient Nonlinear Optical Processes in Semiconductors*, in *Nonlinear Optics in Semiconductors*, edited by R. K. Willardson and A. C. Beers (Academic Press, 1999); J. Shah, *Ultrafast Spectroscopy of Semiconductors and Semiconductor Nanostructures* (Springer, New York, 1996).
- ² S. Schmitt-Rink and D. S. Chemla, Phys. Rev. Lett. **57**, 2752 (1986); S. Schmitt-Rink, D.S. Chemla, and H. Haug, Phys. Rev. B **37**, 941 (1988); M. Lindberg and S. W. Koch, Phys. Rev. B **38**, 3342 (1988); I. Baslev, R. Zimmermann, and A. Stahl, Phys. Rev. B **40**, 4095 (1989).
- ³ R. Binder, S. W. Koch, M. Lindberg, W. Schäfer, and F. Jahnke, Phys. Rev. B **43**, 6520 (1991).
- ⁴ H. Haug and S. W. Koch, *Quantum theory of the optical and electronic properties of semiconductors*, 2nd edition (World Scientific, Singapore, 1993).
- ⁵ P. Kner, S. Bar-Ad, M.V. Marquezini, D.S. Chemla and W. Schäfer, Phys. Rev. Lett. **78**, 1319 (1997); Phys. Stat. Sol. (a) **164**, 579 (1997); P. Kner, W. Schäfer, R. Lövenich, and D. S. Chemla, Phys. Rev. Lett. **81**, 5386 (1998); P. Kner, S. Bar-Ad, M.V. Marquezini, D.S. Chemla, R. Lövenich and W. Schäfer, to appear in Phys. Rev. B (1999).
- ⁶ G. Bartels, A. Stahl, V. M. Axt, B. Haase, U. Neukirch, and J. Gutowski, Phys. Rev. Lett. **81** (1998); B. Haase, U. Neukirch, J. Gutowski, G. Bartels, A. Stahl, V. M. Axt, J. Nürnberger, and W. Faschinger, Phys. Rev. B **59**, R7805 (1999).
- ⁷ A. Schüzgen, R. Binder, M. E. Donovan, M. Lindberg, K. Wundke, H. M. Gibbs, G. Khitrova and N. Peyghambarian Phys. Rev. Lett. **82** 2346 (1999).
- ⁸ T. Aoki, G. Mohs, M. Kuwata-Gonokami and A. A. Yamaguchi, Phys. Rev. Lett. **82** 3108 (1999).
- ⁹ V. Chernyak, S. Yokojima, T. Meier, and S. Mukamel Phys. Rev. B **58**, 4496 (1998).
- ¹⁰ See, e.g., V. M. Axt and S. Mukamel, Rev. Mod. Phys. **70**, 145 (1998) and references therein.
- ¹¹ V. M. Axt and A. Stahl, Z. Phys. B **93**, 195 (1994).
- ¹² Th. Östreich, K. Schönhammer, and L. J. Sham, Phys. Rev. Lett. **74**, 4698 (1995); Phys. Rev. B **58**, 12920 (1998).
- ¹³ See, e.g., H. Haug and A.-P. Jauho, *Quantum Kinetics in Transport and Optics of Semiconductors* (Springer, 1996) and references therein.
- ¹⁴ S. Schmitt-Rink, D. S. Chemla, and D. A. B. Miller, Advances in Physics **38**, 89 (1989).
- ¹⁵ A. Ruckenstein and S. Schmitt-Rink, Phys. Rev. B **35**, 7551 (1987).
- ¹⁶ P. W. Anderson, Phys. Rev. Lett. **18**, 1049 (1967).
- ¹⁷ See, e.g., M. S. Skolnick, J. M. Rorison, K. J. Nash, D. J. Mowbray, P. R. Tapster, S. J. Bass, and A. D. Pitt, Phys. Rev. Lett. **58**, 2130 (1987); G. Livescu, D. A. B. Miller, D. S. Chemla, M. Ramaswamy, T. Y. Chang, N. Sauer, A. C. Gossard, and J. H. English, IEEE Journal of Quantum Electronics **24**, 1677 (1988); W. Chen, M. Fritze, W. Walecki, A. Nurmikko, D. Ackley, M. Hong, L. L. Chang, Phys. Rev. B **45**, 8464 (1992); J. M. Calleja, A. R. Goni, B. S. Dennis, J. S. Weiner, A. Pinczuk, S. Schmitt-Rink, L. N. Pfeiffer, K. West, J. F. Muller, and A. E. Ruckenstein, Solid State Comm. **79**, 911 (1991); M. Fritze, A. Kastalsky, J. E. Cunningham, W. Knox, R. Partak, and I. E. Perakis, Solid State Com. **100**, 497 (1996).
- ¹⁸ K. Ohtaka and Y. Tanabe, Rev. Mod. Phys. **62**, 929 (1990); G. D. Mahan in *Fermi Surface*

- Effects*, ed. J. Kondo and A. Yoshimori (Springer, Berlin), 41 (1988), and references therein.
- ¹⁹ G. D. Mahan, Phys. Rev. **153**, 882 (1967).
- ²⁰ G. D. Mahan, *Many-Particle Physics*, Second Edition (Plenum, 1990).
- ²¹ J. Gavoret, P. Nozieres, B. Roulet, and M. Combescot, J. Phys. (Paris) **30**, 987 (1969).
- ²² K. Ohtaka and Y. Tanabe, Phys. Rev. B **39**, 3054 (1989).
- ²³ T. Uenoyama and L. J. Sham, Phys. Rev. Lett. **65**, 1048 (1990).
- ²⁴ P. Hawrylak, Phys. Rev. B **44**, 3821 (1991).
- ²⁵ See e.g. R. F. Bishop and H. G. Kummel, Physics Today p. 52 (March 1987); H. Kummel, K. H. Luhrmann, and J. G. Zabolitzky, Phys. Rep. **36**, 3 (1978); R. F. Bishop, Theor. Chim. Acta **80**, 95 (1991); J. Arponen, Ann. Phys. (N. Y.) **151**, 311 (1983).
- ²⁶ K. Schönhammer and O. Gunnarsson, Phys. Rev. B **18**, 6606 (1978).
- ²⁷ I. E. Perakis and Yia-Chung Chang, Phys. Rev. B **44**, 5877 (1991); *ibid* **43**, 12556 (1991); Proc. 20th Int. Conf. Phys. Sem., eds E. M. Anastassakis and J. D. Joannopoulos (World Scientific, Singapore) 1109 (1990).
- ²⁸ I. E. Perakis and Yia-Chung Chang, Phys. Rev. B **47**, 6573 (1993).
- ²⁹ K. Emrich and J. G. Zabolitzky, Phys. Rev. B **30**, 2049 (1984); R. F. Bishop and K. H. Luhrmann, Phys. Rev. B **17**, 3757 (1978); *ibid.* **26**, 5523 (1982).
- ³⁰ J. W. Negele, Rev. of Mod. Phys. **54**, 913 (1982).
- ³¹ H. Wang, J. Shah, T. C. Damen, S. W. Pierson, T. L. Reinecke, L. N. Pfeiffer, and K. West, Phys. Rev. B **52**, R17013 (1995).
- ³² W. H. Knox, D. S. Chemla, G. Livescu, J. E. Cunningham, and J. E. Henry, Phys. Rev. Lett. **61**, 1290 (1988).
- ³³ D-S Kim, J. Shah, J. E. Cunningham, T. C. Damen, S. Schmitt-Rink, and W. Schäfer, Phys. Rev. Lett. **68**, 2838 (1992).
- ³⁴ See e.g. R. H. M. Groeneveld, R. Sprik, A. Lagendijk, Phys. Rev. B **51**, 11433 (1995); C. K. Sun, F. Vallee, L. H. Acioli, E. P. Ippen, and F. G. Fujimoto, Phys. Rev. B **50**, 15337 (1994); W. S. Fann, R. Storz, W. H. K. Tom, and J. Bokor, Phys. Rev. B **46**, 13592 (1992); H. Petek, A. P. Heberle, W. Nessler, H. Nagano, S. Kubota, S. Matsunami, N. Moriya, and S. Ogawa, Phys. Rev. Lett. **79**, 4649 (1997); J.-Y. Bigot, J.-C. Merle, O. Cregut, and A. Daunois, Phys. Rev. Lett. **75**, 4702 (1995); T. V. Shahbazyan, I. E. Perakis, and J.-Y. Bigot, Phys. Rev. Lett. **81**, 3120 (1998).
- ³⁵ D. Pines and P. Nozieres, *The Theory of Quantum Liquids* (Addison-Wesley, 1989).
- ³⁶ P. Hawrylak, J. F. Young, and P. Brockmann, Phys. Rev. B **49**, 13624 (1994).
- ³⁷ I. Brener, W. H. Knox, and W. Schaefer, Phys. Rev. B **51**, 2005 (1995).
- ³⁸ I. E. Perakis, I. Brener, W. H. Knox, and D. S. Chemla, J. Opt. Soc. Am. B **13**, 1313 (1996); *Ultrafast Phenomena IX*, eds P. F. Barbara, W. H. Knox, G. A. Mourou, and A. H. Zewail, p. 407 (Springer-Verlag, Berlin, 1994).
- ³⁹ I. E. Perakis and T. V. Shahbazyan, Int. J. Mod. Phys. B **13**, 869 (1999).
- ⁴⁰ L. Allen and J. H. Eberly, *Optical Resonance and Two-Level Atoms* (Dover, New York 1987).
- ⁴¹ J. R. Schrieffer, J. Appl. Phys. **38**, 1143 (1967); I. Shavitt and L. Redmon, J. Chem Phys. **73**, 5711 (1980); and references therein.
- ⁴² C. Cohen-Tannoudji, J. Dupont-Roc, and G. Grynberg, *Atom-Photon Interactions: Basic Processes and Applications* (John Wiley & Sons, Inc., 1992).

- ⁴³ E. Müller-Hartmann, T. V. Ramakrishnan, and G. Toulouse, Phys. Rev. B **3**, 1102 (1971).
- ⁴⁴ A good discussion of the physics may be found in G. D. Mahan, Solid State Phys. **29**, ed. H. Ehrenreich, F. Seitz, and D. Turnbull (Academic, New York) 75 (1974).
- ⁴⁵ P. W. Anderson, Phys. Rev. **112**, 1900 (1958); D. Pines, *Elementary Excitations in Solids* (Addison-Wesley, 1963).
- ⁴⁶ P. Hawrylak, Phys. Rev. B **42**, 8986 (1990).
- ⁴⁷ K. El Sayed, S. Schuster, H. Haug, F. Herzel, and K. Hennerberger, Phys. Rev. B **49**, 7337 (1994).
- ⁴⁸ L. Bányai, Q. T. Vu, B. Mieck, and H. Haug, Phys. Rev. Lett. **81**, 882 (1998).
- ⁴⁹ See, e.g., J. Igarashi, J. Phys. Soc. Jpn **54**, 260 (1985).
- ⁵⁰ I. E. Perakis and D. S. Chemla, Phys. Rev. Lett. **72**, 3202 (1994); I. E. Perakis, Chem. Phys. **210**, 259 (1996).
- ⁵¹ W. Knox, D. S. Chemla, D. A. B. Miller, J. Stark, and S. Schmitt-Rink, Phys. Rev. Lett. **62**, 1189 (1989).
- ⁵² D.S. Chemla, W.H. Knox, D.A.B. Miller, S. Schmitt-Rink, J.B. Stark, and R. Zimmermann, J. Lumin. **44**, 233 (1989).
- ⁵³ C. Ell, J. F. Muller, K. El Sayed, and H. Haug, Phys. Rev. Lett. **62**, 304 (1989); O. Betbeder-Matibet, M. Combescot, and C. Tanguy, Phys. Rev. B **44**, 3762 (1991).

FIGURES

FIG. 1. The effect of the pump pulse on the band dispersion, $\varepsilon_{\mathbf{k}}(t) = \varepsilon_{\mathbf{k}}^c(t) + \varepsilon_{-\mathbf{k}}^v(t)$, of the “pump-dressed” system. Solid line: “bare” dispersion ($t = -\infty$). Dashed line: pump-renormalized dispersion ($t = 0$). The bands become “heavier” for the duration of the pump.

FIG. 2. (a) The e - h scattering processes that contribute to the rhs of Eq. (25). Full lines correspond to $s(\mathbf{p}, \mathbf{k}, t)$ and thin lines to V . The diagrams describe (from top to bottom) (i) Born scattering of a FS electron, (ii) FS electron ladder diagrams, (iii) FS hole ladder diagrams, and (iv) Nonlinear vertex corrections due to the dynamical FS response. (b) Scattering processes state that determine the time- and momentum-dependence of the effective e - h potential $\tilde{V}(\mathbf{p}, t)$ and lead to the unbinding of the HFA bound state.

FIG. 3. Linear absorption resonance lineshape for FES (solid curve) compared to the HFA (dashed curve), calculated with $g = 0.4$ and $\Gamma = 0.1E_F$. The HFA resonance position was shifted for better visibility.

FIG. 4. The absorption spectra for the FES (a) compared to the HFA (b). Solid curves: linear absorption. Dashed curves: nonlinear absorption. The curves were calculated with $g = 0.4$ and $\Gamma = 0.1E_F$ at time delay $\tau = -0.1\Gamma^{-1} = -t_p/2$ and pulse duration $t_p = 2.0E_F^{-1}$. The nonlinear absorption lineshapes exhibit bleaching, resonance blueshift, and gain below the absorption onset that differ in the two cases.

FIG. 5. Differential transmission lineshape for various time delays calculated with $g = 0.4$, $\Gamma = 0.1E_F$, and $t_p = 2.0E_F^{-1}$. (a) Long time delay, $\tau = -1.5\Gamma^{-1} = -15.0E_F^{-1}$. For the FES, the oscillations in the differential transmission spectra are reduced (solid curve) as compared to the HFA (dashed curve). (b) Short time delay, $\tau = -0.1T_2 = -t_p/2 = -1.0E_F^{-1}$. For the FES, the differential transmission spectrum is asymmetric (solid curve) as compared to the symmetric lineshape for the HFA (dashed curve). The above curves were shifted for better visibility.

FIG. 6. (a) Nonlinear absorption resonance bleaching evaluated at the instantaneous peak frequency as function of time delay for the FES (solid curve) compared to the HFA (dashed curve). The curves were calculated with $g = 0.4$, $\Gamma = 0.1E_F$, and $t_p = 2.0E_F^{-1}$. The time-dependence of the pump pulse is also presented for comparison (dotted curve). (b) Same calculated using the rigid band shift model, Eq. (34).

FIG. 7. The enhancement of the nonlinear absorption resonance of the FES (dashed curve) vs. linear absorption (solid curve) at long time delay $\tau = -1.5\Gamma^{-1}$. The curves were calculated with $g = 0.4$, $\Gamma = 0.1E_F$, and $t_p = 2.0E_F^{-1}$.

FIG. 8. Nonlinear absorption resonance blueshift as function of time delay for the FES (solid curve) compared to the HFA (dashed curve). The blueshift is significantly weaker for the HFA. The curves were calculated with $g = 0.4$, $\Gamma = 0.1E_F$, and $t_p = 2.0E_F^{-1}$. The time-dependence of the pump pulse is also presented for comparison (dotted curve).

FIG. 9. Resonance bleaching as function of time delay for the FES (a) compared to the HFA (b) for different strengths of the e - h interaction: $g=0.4$ (solid curve) and $g=0.3$ (dashed curve). The curves were calculated with $\Gamma = 0.1E_F$, and $t_p = 2.0E_F^{-1}$. The time-dependence of the pump pulse is also presented for comparison (dotted curve).

FIG. 10. The effect of the pump-induced renormalization of the band dispersions on the e - h interactions. The function $F(\omega, \tau)$, given by Eq. (35), for the FES (a) compared to the HFA (b) in the presence (dashed curve) and absence (solid curve) of the pump pulse. The curves were calculated with $g = 0.4$, $\Gamma = 0.1E_F$, and $t_p = 2.0E_F^{-1}$.

FIG. 11. The effect of the pump-induced renormalization of the band dispersions on the resonance strength. The nonlinear absorption spectrum for the FES (a) compared to the HFA (b). Solid curves: Linear absorption. Dashed curves: Nonlinear absorption. Dotted curves: Nonlinear absorption for a rigid band shift only. The curves were calculated with $g = 0.4$, $\Gamma = 0.1E_F$, and $t_p = 2.0E_F^{-1}$.

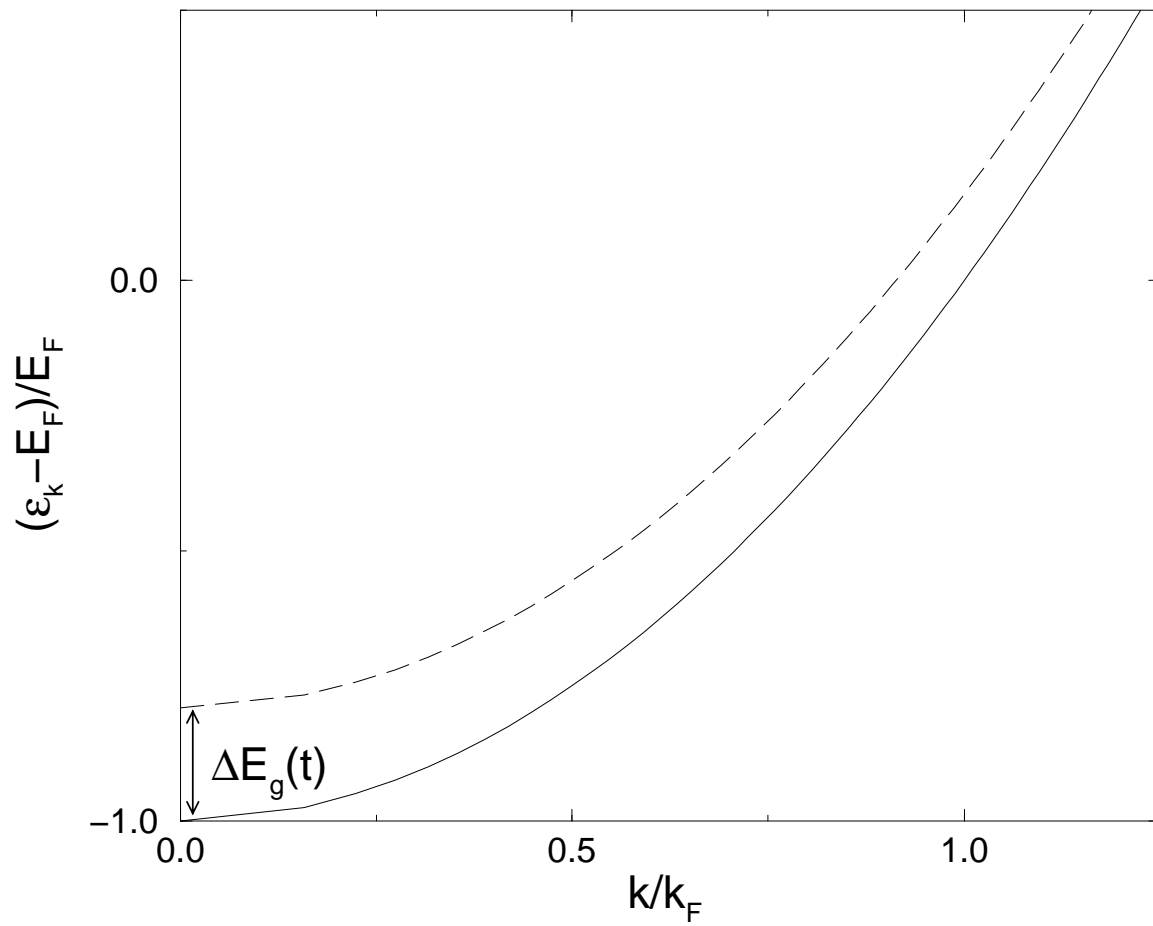
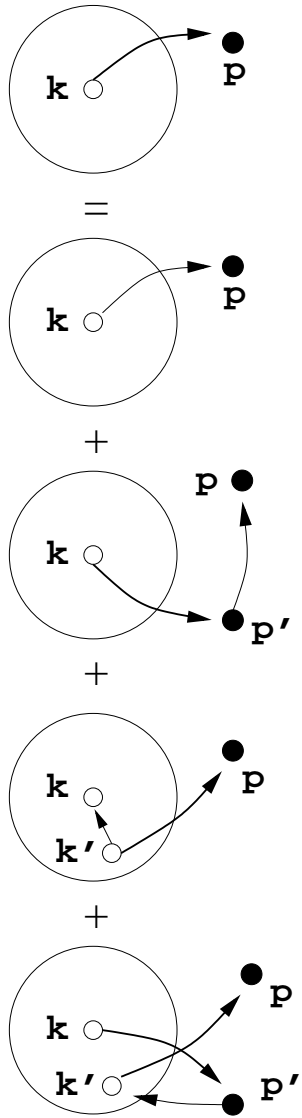


FIG. 1

(a)



(b)

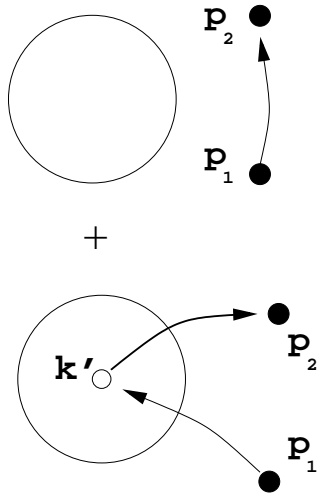


FIG. 2

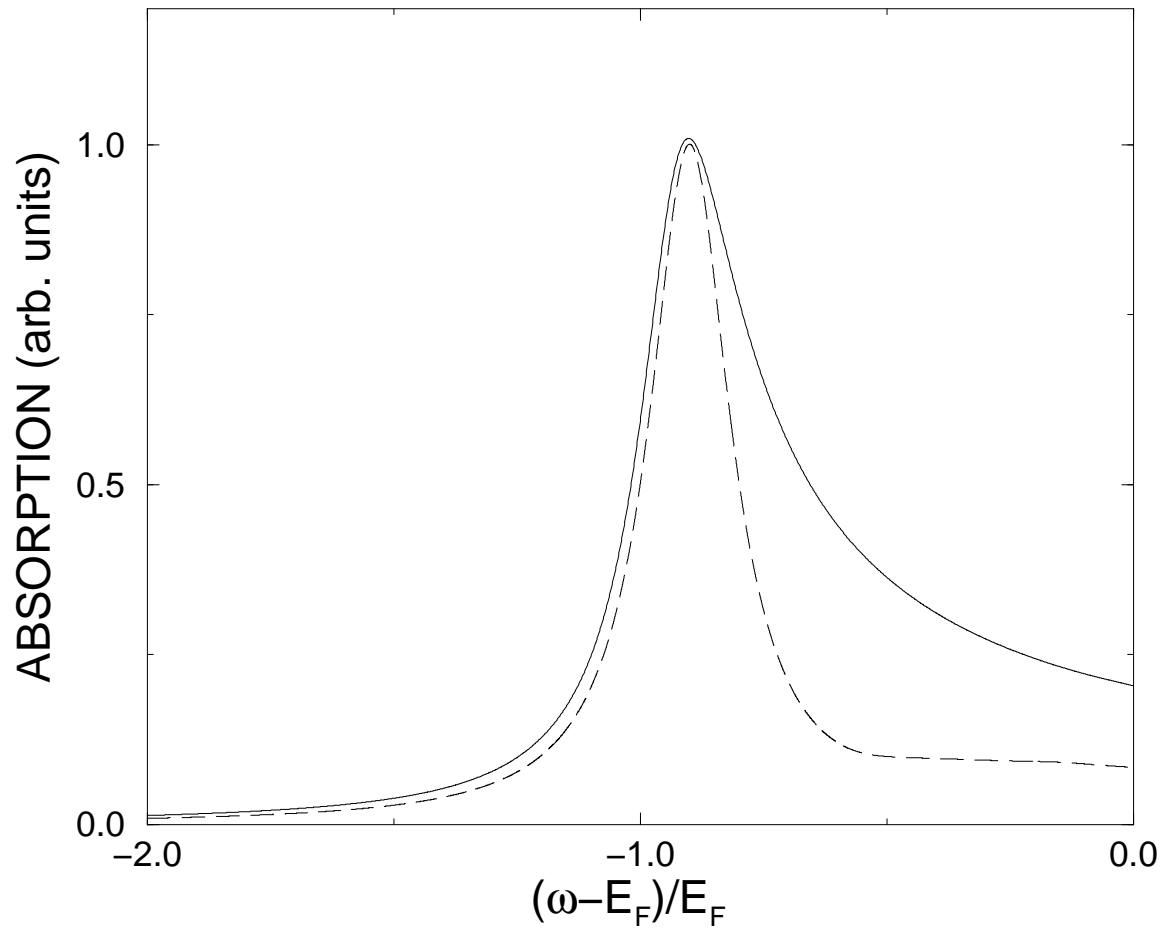


FIG. 3

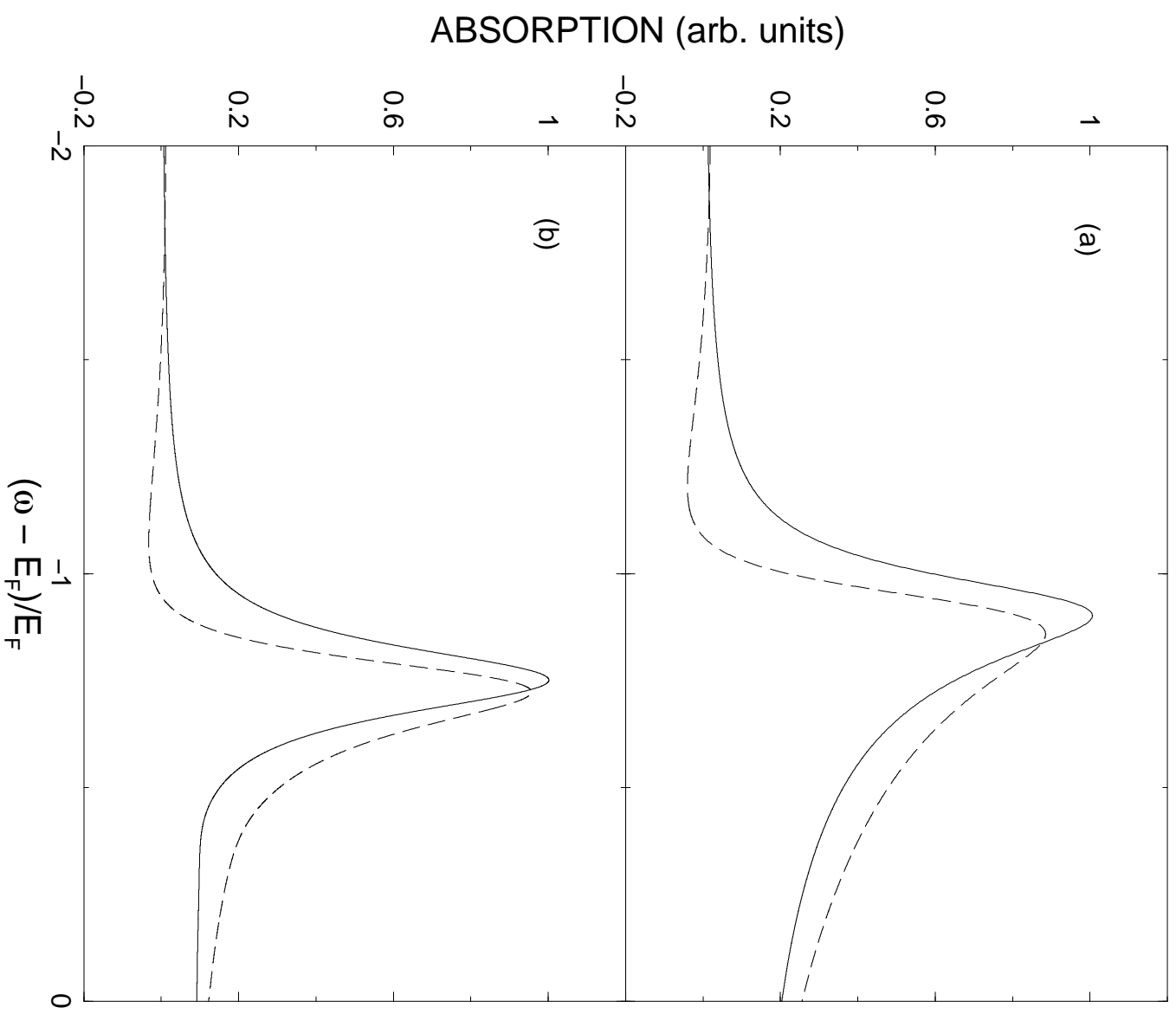


FIG. 4

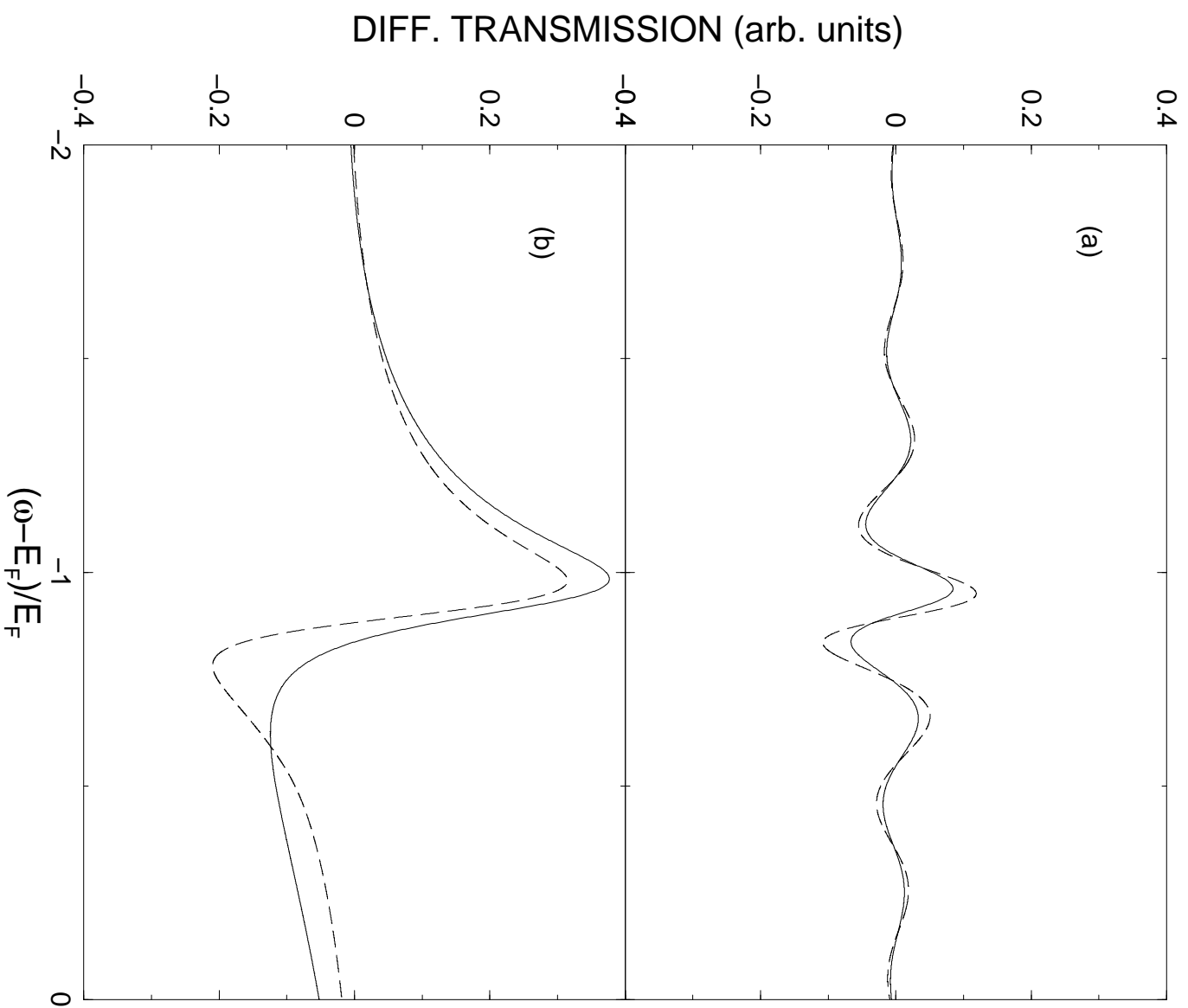


FIG. 5

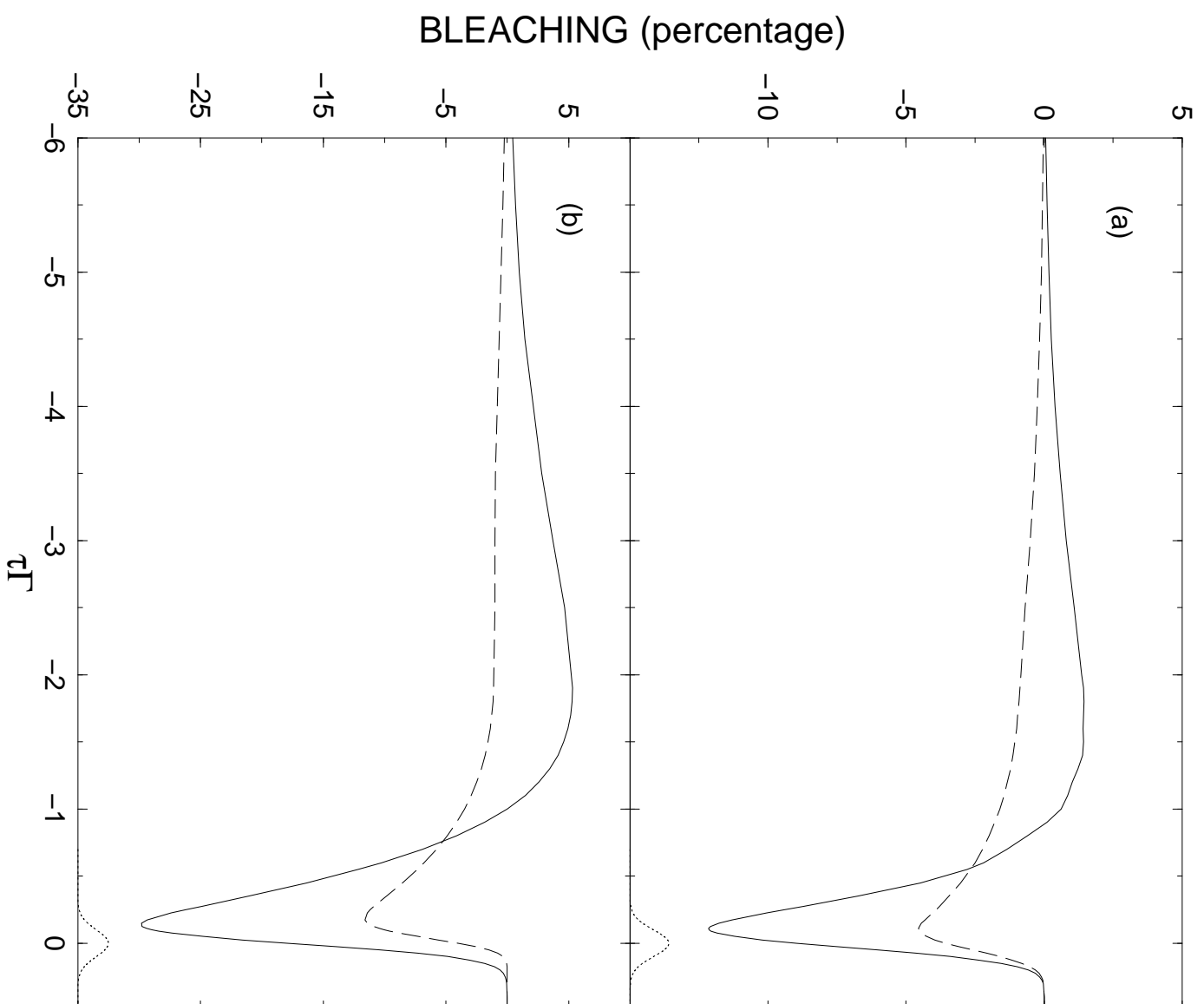


FIG. 6

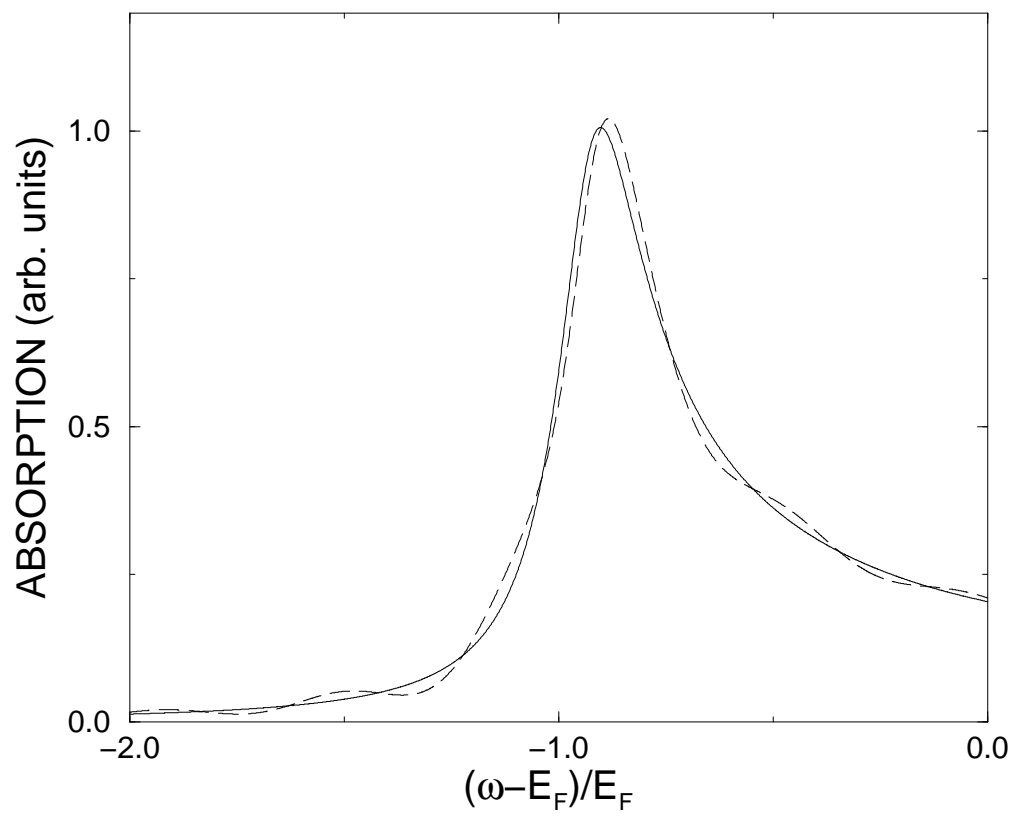


FIG. 7

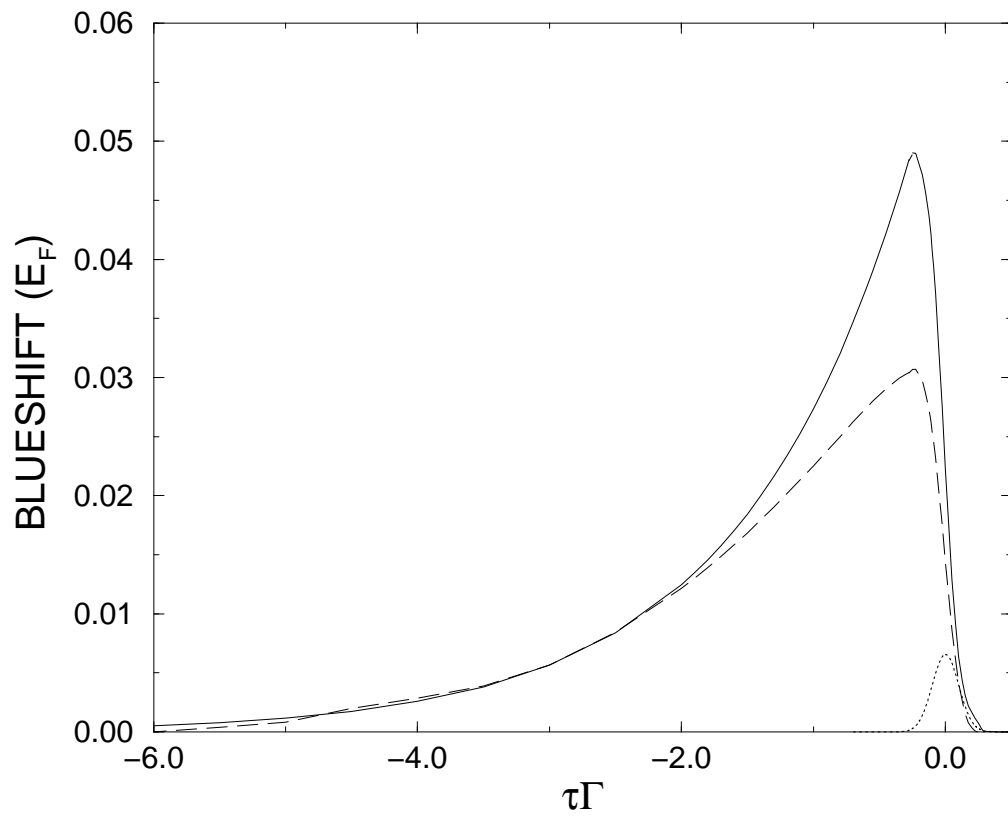


FIG. 8

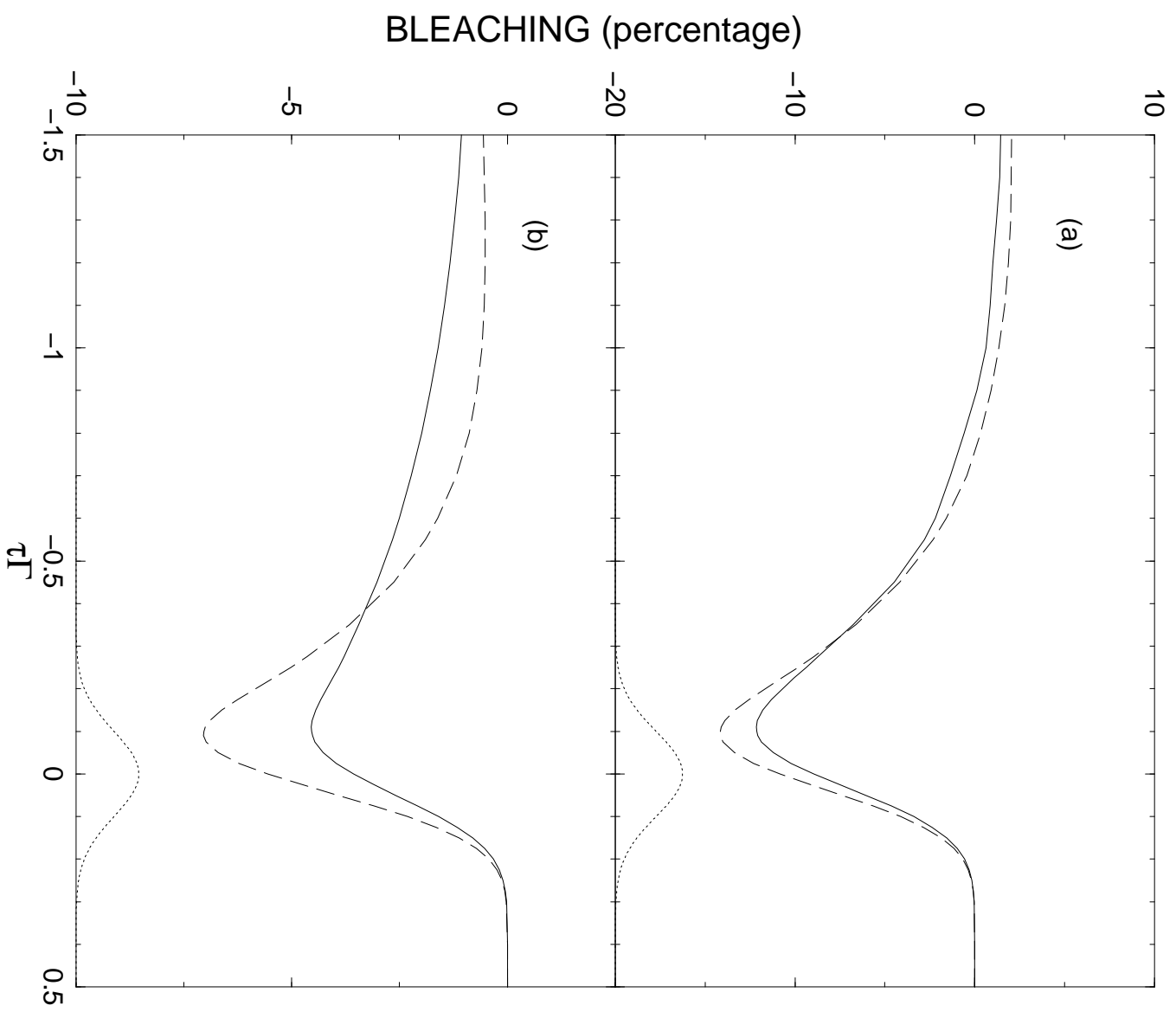


FIG. 9

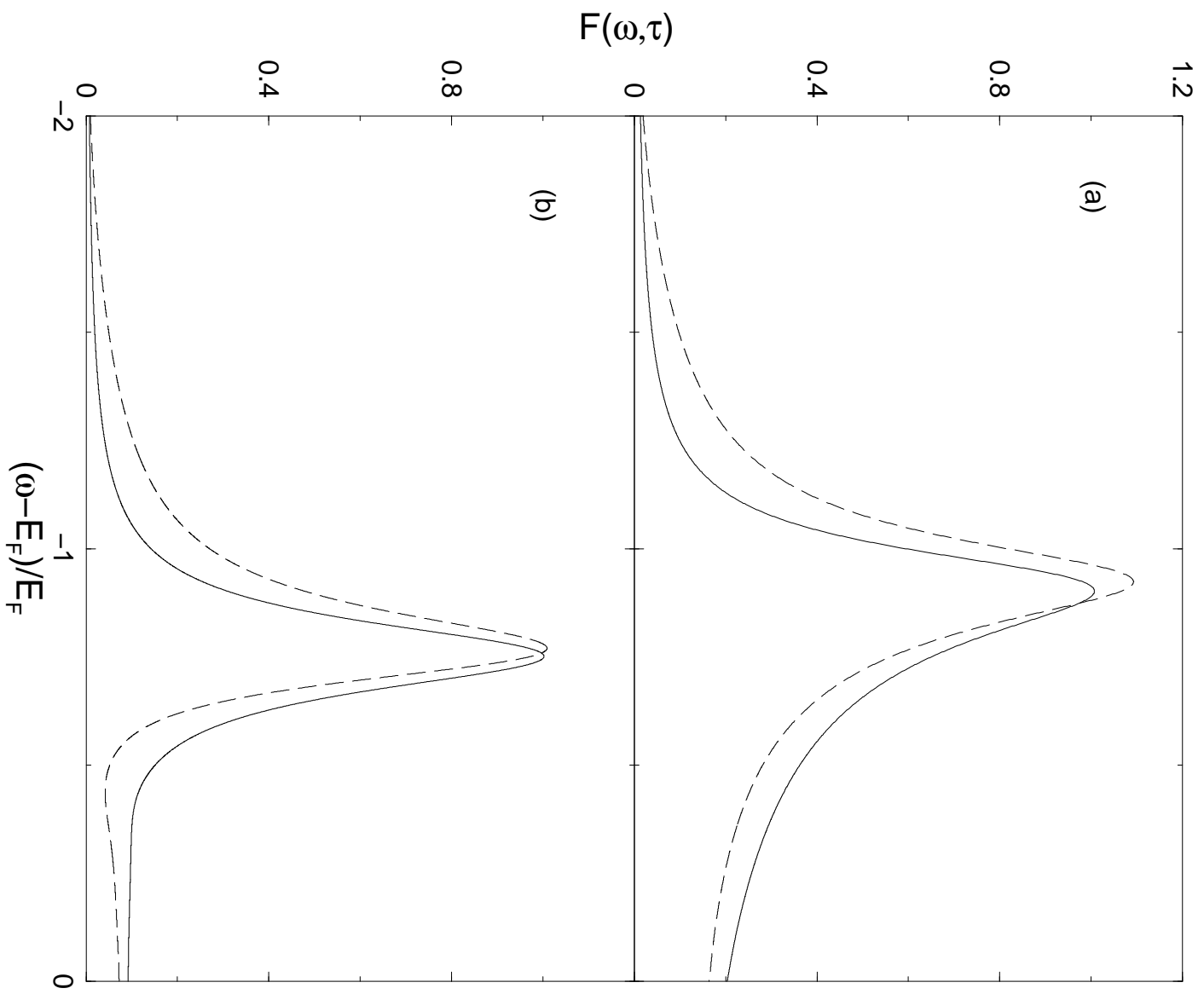


FIG. 10

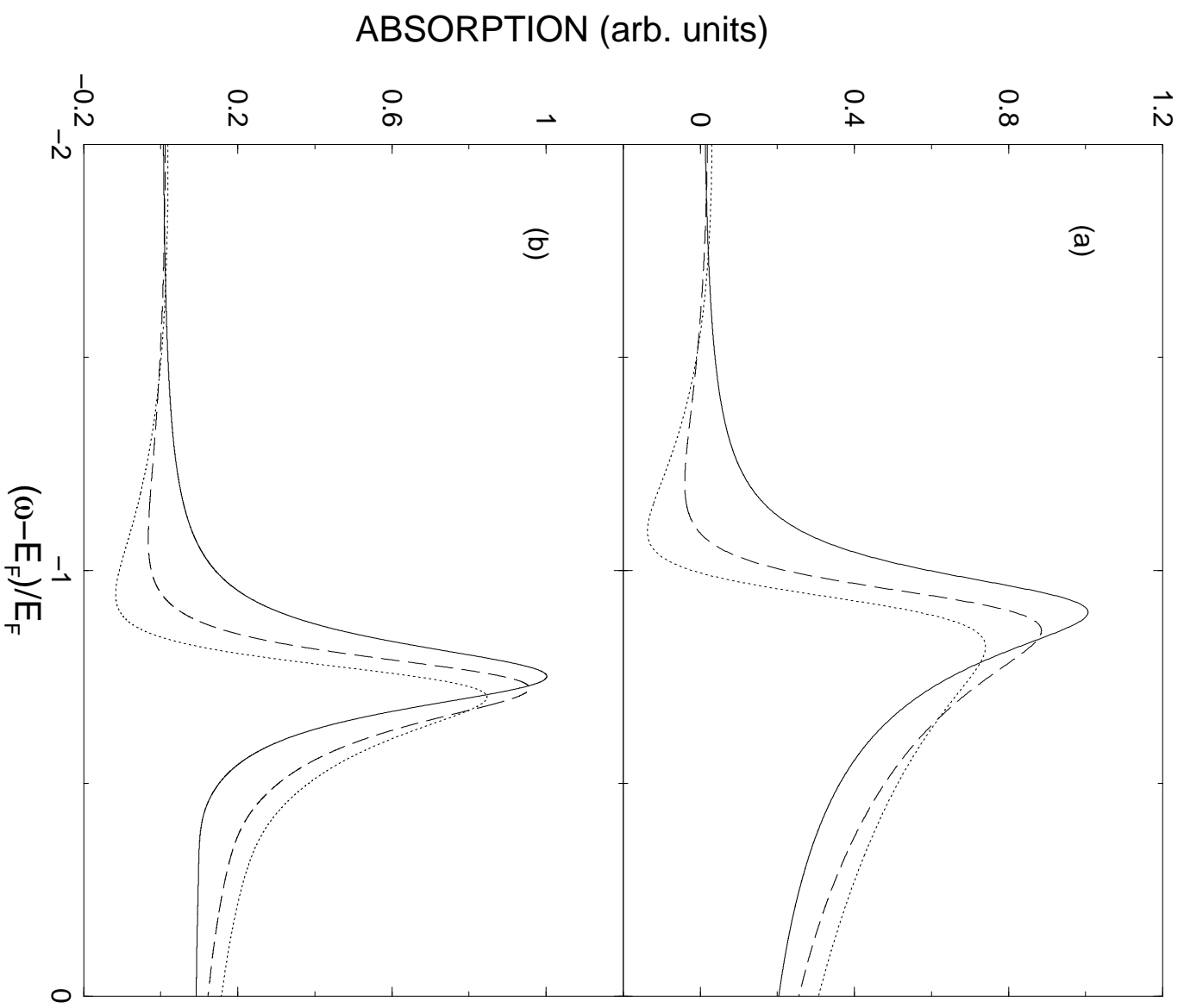


FIG. 11